# OPTIMIZING THE SUBSTRATE FOR MATURING HUMAN EMBRYONIC STEM CELL DERIVED RETINAL PIGMENT EPITHELIUM

Pyry Grönroos

Master's Thesis

University of Tampere

Faculty of Medicine and Life Sciences

19.1.2017

# ACKNOWLEDGEMENTS

This master's thesis was carried out in the Eye group, Faculty of Medicine and Life Sciences, University of Tampere between March 2015 and October 2015. First, I would like to express my sincere gratitude for the group leader Heli Skottman, for creating the opportunity to participate in such interesting project.

I would like to highly acknowledge my supervisor Tanja Ilmarinen for her professional and exceptionally good guidance through the whole thesis process. I have learned a great deal from her about high quality research in laboratory as well as doing the writing process. I would also thank Anni Sorkio and Elina Vuorimaa-Laukkanen for the assistance with complicated laboratory apparatuses used in Tampere University of Technology. Furthermore, I like to thank technicians Outi Melin and Hanna Pekkanen for their assistance and counsel in laboratory issues. Finally, I want to thank the other Eye group members for inspiring working atmosphere and all the help they provided.

# PRO GRADU –TUTKIELMA


| | |
|---|---|
| Paikka: | Tampereen yliopisto, Lääketieteen ja biotieteiden tiedekunta |
| Tekijä: | GRÖNROOS, PYRY |
| Otsikko: | Kasvualustan optimointi kypsyvälle ihmisen alkion kantasoluista erilaistetulle verkkokalvon pigmenttiepiteelille |
| Sivumäärä: | 61 |
| Ohjaaja: | FT Tanja Ilmarinen |
| Tarkastajat: | Apulaisprofessori Heli Skottman ja FT Tanja Ilmarinen |
| Päiväys: | 19.1.2017 |


# TIIVISTELMÄ


**Taustatieto ja tavoitteet** Verkkokalvon pigmenttiepiteelisolut muodostavat yksinkertaisen epiteelin, joka sijaitsee Bruchin kalvon päällä, silmän neuraalisen retinan ja suonikalvon välissä. Sillä on erittäin tärkeitä näkökyvyn ylläpitämiseen ja kudosten suojaamiseen liittyviä tehtäviä. Silmäpohjan ikärappeuma ja monet muut verkkokalvon sairaudet, joille ei ole vielä löydetty tehokasta hoitoa, johtuvat usein toimintahäiriöistä pigmenttiepiteelissä. Pluripotenteista kantasoluista erilaistetut verkkokalvon pigmenttiepiteelisolut on mahdollista siirtää vahingoittuneen tilalle. Jotta kliinisiä sovelluksia päästään toteuttamaan, tarvitaan vielä lisätutkimusta ja optimointia. Solujen kasvualustan ja olosuhteiden pitää muistuttaa niille luontaista soluväliainetta, jotta ne kypsyvät onnistuneesti. Tässä tutkimuksessa vertailtiin ja optimoitiin erilaisia kasvualustojen materiaaleja, päällystysmenetelmiä ja proteiineja, sekä tutkittiin niiden vaikutuksia pluripotenteista kantasoluista erilaistettujen verkkokalvon pigmenttiepiteelisolujen kypsymiseen. Työn tavoitteena oli löytää kypsyville soluille parempi kasvualusta vanhan ja heikoksi havaitun protokollan tilalle.

**Menetelmät** Tässä tutkimuksessa oli kaksi vaihetta. Ensimäisessä vaiheessa laminiini 521:stä (L521) päällystettiin Langmuir-Schaefer (LS) tekniikalla polyetyleenitereftalaatti (PET) ja polyimidi (PI) kalvoille. Tämän jälkeen kalvoille päällystetyn laminiinin polymerisoitumista tarkkailtiin immunovärjäyksin. Seuraavaksi päällystetyille kalvoille siirrettiin kantasoluista erilaistettuja verkkokalvon pigmenttiepiteelisoluja, joiden tarttumista, leviämistä ja pigmentoitumista seurattiin kahdeksan viikkoa, jonka jälkeen solut karakterisoitiin immunofluoresenssivärjäyksillä konfokaalimikroskoopilla. Toisessa vaiheessa etsittiin parasta kasvualustaa uitto-päällystys menetelmällä. Kasvualustan proteiineina toimi kollageeni tyyppi IV (C-IV), L521 ja nidogeeni-1 (Nid), joiden eri kombinaatioita ja konsentraatioita testattiin PET inserteillä. Soluja kasvatettiin näytteiden päällä 9-15 viikkoa. Päällystetyt näytteet ja solut analysoitiin kuten ensimäisessä vaiheessa.

**Tulokset** LS-tekniikalla päällystetty L521 osoitti polymerisoitumista erityisesti PI-kalvolla. Solut kasvoivat sekä LS-PET ja LS-PI kalvoilla ilmentäen verkkokalvon epiteelisoluille ominaisia immunomarkkereita, mutta kypsyminen osoittautui hitaammaksi verrattuna uitto-päällystettyyn näytteisiin. Proteiinikombinaatioissa C-IV ja L521 yhdistelmä osoittautui merkittävästi paremmaksi kuin aiemmin käytetty pelkkä C-IV. Mitä suurempi konsentraatio Nid:ä kombinaatiossa, sitä voimakkaampi pigmentaatio ja tiettyjen immunomarkkerien ekspressio. Suuret Nid määrät aiheutti kuitenkin soluaggregaatteja ja epätasaisuutta.

**Johtopäätökset** LS-tekniikka osoittautui lupaavaksi päällystysmenetelmäksi polymerisoiden laminiinia, mutta vaatii vielä paljon lisätutkimusta. Uitto-päällystetyissä näytteissä C-IV + L521 kombinaatio oli ylivertainen aikaisempaan C-IV päällystykseen. Nidogeenin määrä parantaa kypsymistä, mutta aiheuttaa suurina määrinä sivuvaikutuksia.

# MASTER'S THESIS


| | |
|---|---|
| Place: | University of Tampere, Faculty of Medicine and Life Sciences |
| Author: | GRÖNROOS, PYRY |
| Title: | Optimizing the substrate for maturing human embryonic stem cell derived retinal pigment epithelium |
| Pages: | 61 |
| Supervisor: | PhD Tanja Ilmarinen |
| Reviewers: | Associate professor Heli Skottman and PhD Tanja Ilmarinen |
| Date: | 19.1.2017 |


# ABSTRACT


**Background and aim** Retinal pigment epithelium (RPE) is a monolayer, which lies on Bruch's membrane (BM) between neural retina and choriocapillaris. RPE has very important role maintaining vision and protecting underlying tissues. Age-related macular degeneration and other retinal disorders are often caused by RPE dysfunction, and there is no effective treatment available for them so far. However, human pluripotent stem cell (hPSC) derived RPE cells can be transplanted to damaged retina providing a potential new treatment. Before heading to clinical applications, further research and optimization is needed. To mature hPSC-RPE cells successfully *in vitro*, the substrate and environment must mimic the natural extracellular matrix such as BM. This study pursued to optimize the best substrate for maturing hPSC-RPE cells using different coating protocols, materials and proteins. The aim of this project was to find better coating method for previously used one, which has unsatisfactorily supported hPSC-RPE attachment, proliferation and maturation.

**Methods** There were two major phases in this study. First, laminin 521 (L521) was coated with Langmuir-Schaefer (LS) method on polyethylene terephthalate (PET) and polyimide (PI) membranes. The successfulness of the coatings and L521 polymerization was investigated with immunostainings. Next, hPSC-RPE cells were passaged to the coatings and their attachment, spreading and pigmentation were observed for eight weeks. Finally, the cells were characterized with immunocytochemical stainings using confocal microscope z-stacks. In the second phase, the best substrate was searched with dip-coat (DC) method using collagen type IV (C-IV), L521 and nidogen-1 (Nid) as coating proteins. Different combinations of these proteins were tested on PET inserts. Cells were cultured on substrates 9-15 weeks. Dip-coatings and hPSC-RPE cells were analyzed and characterized as in first phase.

**Results** LS-coated L521 showed polymerization, especially on PI-membrane. hPSC-RPE cells grew on both LS-PET and LS-PI membranes expressing many crucial RPE immunomarkers. However, the maturation turned out to be slower compared to DC sample. C-IV + L521 proved to be superior DC substrate combination compared to previously used simple C-IV coating. Furthermore, adding different concentrations of Nid to the combination increased progressively pigmentation and some of the immunomarker expressions. However, high Nid concentrations caused cell aggregates and erratic monolayer.

**Conclusions** LS-technicque turned out to be a potential coating method by polymerizing laminin, but much more research and resources are still needed. DC C-IV + L521 combination was superior compared to simple C-IV and the addition of Nid improves the maturation, however higher amounts of Nid cause adverse effects.

# TABLE OF CONTENTS


**1. INTRODUCTION ..... 1**

**2. REVIEW OF LITERATURE ..... 2**

2.1 RETINAL PIGMENT EPITHELIUM ..... 2

2.1.1 *The structure of the eye and retina* ..... 2

2.1.2 *Retinal pigment epithelium cells* ..... 3

2.1.3 *Characterization of RPE cells* ..... 4

2.1.4 *Retinal degeneration* ..... 5

2.1.5 *Cell replacement therapies* ..... 7

2.2 PSCs AS SOURCE FOR RPE CELLS ..... 8

2.2.1 *Human pluripotent stem cells* ..... 8

2.2.2 *Differentiation of hPSCs towards RPE cells* ..... 10

2.3 CELL MATERIAL INTERACTION ..... 11

2.3.1 *Protein adsorption and cell spreading* ..... 11

2.3.2 *Material characteristics* ..... 13

2.4 COATING METHODS AND SUBSTRATES ..... 14

2.4.1 *Laminin* ..... 15

2.4.2 *Collagen IV* ..... 15

2.4.3 *Nidogen* ..... 16

2.4.4 *Langmuir-Schaefer coating* ..... 16

**3. AIMS OF THE STUDY ..... 18**

**4. MATERIALS AND METHODS ..... 19**

4.1 CELL CULTURE ON DIFFERENT COATING MATERIALS ..... 19

4.1.1 *DC protocol* ..... 19

4.1.2 *Langmuir-Schaefer protocol* ..... 19

4.1.3 *Cell material* ..... 20

4.1.4 *hPSC-RPE culture to the coated substrates* ..... 20

4.2 CHARACTERIZATION OF COATING AND CELL MATURATION ..... 21

4.2.1 *Detection of protein coating deposition by immunocytochemistry* ..... 21

4.2.2 *Intensity test* ..... 22

4.2.3 *Characterization of hPSC-RPE by immunocytochemistry* ..... 22

4.2.4 *Transepithelial resistance*..... **Error! Bookmark not defined.**
**5. RESULTS..... 24**
5.1 CELL CULTURE ON LANGMUIR-SCHAEFER AND DIP-COATED LAMININ 24
5.1.1 *Deposition of the coating proteins*..... 24
5.1.2 *Cell attachment and growth of hESC-RPE on LS-coating*..... 26
5.1.3 *Characterization of hESC-RPE on LS-coating with immunocytochemistry* .... 27
5.2 CELL CULTURE ON DIP-COATED PROTEIN COMBINATIONS..... 29
5.2.1 *Deposition of the protein combinations using dip-coating technique*..... 29
5.2.2 *Cell attachment and growth of hESC-RPE on DC combinations* ..... 30
5.2.3 *Chracterization of DC hESC-RPE with immunocytochemistry* ..... 33
**6. DISCUSSION ..... 36**
6.1 CELL CULTURE ON LANGMUIR-SCHAEFER AND DIP-COATED LAMININ 36
6.2 CELL CULTURE ON DIP-COATED PROTEIN COMBINATIONS..... 38
**7. CONCLUSION..... 42**
**REFERENCES..... 43**
**APPENDIX ..... 49**

# ABBREVIATIONS

| | |
|---|---|
| A488 | Alexa Fluor 488 |
| A568 | Alexa Fluor 568 |
| AMD | Age-related macular degeneration |
| BEST1 | Bestrophin |
| bFGF | basic fibroblast growth factor |
| BM | Bruch's membrane |
| BSA | Bovine serum albumin |
| BVMD | Best vitelliform macular dystrophy |
| C-IV | Collagen type IV |
| CL | Collagen |
| CL-I | Collagen I |
| CRALBP | Cellular retinaldehyde-binding protein |
| DAPI | 4',6-diamidino-2-phenylidole |
| DC | Dip-coating |
| DM- | hPSC-RPE culture medium |
| DMEM/12 | Dulbecco's Modified Eagle Medium: Nutrient Mixture F-12 |
| DPBS | Dulbecco's Phosphate Buffered Saline |
| ECM | Extracellular matrix |
| ESC | Embryonic stem cell |
| GMP | Good manufacturing practice |
| hESC | Human embryonic stem cell |
| hiPSC | Human induced pluripotent stem cell |
| hPSC | Human pluripotent stem cell |
| ICM | Inner cell mass |
| iPSC | Induced pluripotent stem cell |
| IgG | Immunoglobulin G |
| IVF | *In vitro* fertilization |
| KO-DMEM | Knock-Out Dulbecco's Modified Eagle Medium |
| KO-SR | Knockout serum replacement |
| L521 | Laminin 521 |
| LB | Langmuir-Blodgett |
| LN | Laminin |
| LS | Langmuir-Schaefer |
| MEFs | Mouse embryonic fibroblasts |
| MERTK | Proto-oncogene tyrosine-protein kinase MER |
| NEAA | Non-essential Amino Acids |
| Nid | Nidogen |
| PEDF | Pigment epithelium-derived factor |
| PET | Polyethylene terephthalate |
| PI | Polyimide |
| PLC | Perlecan |
| POS | Photoreceptor outer segments |
| PSC | Pluripotent stem cell |
| RP | Retinitis pigmentosa |
| RPC | Retinal progenitor cell |
| RPE | Retinal pigment epithelium |

| | |
|---|---|
| RPE65 | Retinal pigment epithelium-specific protein 65 kDa |
| RT | Room temperature |
| TER | Transepithelial resistance |
| TEO | The National Authority for Medicolegal Affairs Finland |
| VEGF | Vascular endothelial growth factor |
| ZO-1 | Zonula occludens-1 |

# 1. INTRODUCTION

Human pluripotent stem cells (hPSC) are capable of unlimited proliferation without undergoing differentiation, and at the same time having the potential to differentiate into any cell type (Reubinoff et al. 2000). Using them as a new approach to treat variety of diseases and defects has become more and more common in the modern era.

Retinal pigment epithelium (RPE) is the outermost layer of the retina, which is a complex and layered structure lining the inner surface of the eye. It is a monolayer of cuboid epithelial cells that lies on the Bruch's membrane (BM). RPE has some very essential functions for normal vision such as light absorption, secretion of growth factors and participation in the visual cycle. (Strauss, 2005) Epithelial cells such as RPE are constantly interacting with the surrounding extracellular matrix (ECM), which provides structural support for the cells and regulates the cell behavior with soluble growth factors. Especially, the ECM plays a vital role in the determination, differentiation, proliferation, survival, polarity and migration of the cells. (Hynes, 2009)

Degenerative retinal diseases including age-related macular degeneration (AMD), Best's disease and retinitis pigmentosa (RP) are often linked to dysfunctional RPE. Currently, there are no effective treatment options for these diseases, not to mention that there is chronic shortage of donor tissues. However, ongoing stem cell research can provide a new source of tissue for replacement therapies, once the protocols and methods are entirely optimized. It has been already proven that hPSC can be differentiated to functional RPE cells (Vaajasaari et al. 2011), but the substrate that mimics properly natural BM is still under research. The most crucial substrate proteins in BM are collagen type IV (C-IV) and laminin (LN) (Booij et al. 2010), which are also the main elements that will be experimented in this study.

Our research group has been using C-IV with dip-coating (DC) method for maturing hPSC-RPE cells (Sorkio et al. 2014), but the cell attachment, spreading and morphology became unsatisfying with varying outcomes, especially after cryopreservation. The need of new coating protocol was imminent. The aim of this study was to polymerize LN for coating purposes with Langmuir-Schaefer (LS) technique, which is following the Sorkio et al. (2015) research with LS-coatings using C-IV and Collagen I (CL-I). Futhermore, the cornerstone of this study was to find the best *in vitro* cell culture substrate for maturing hPSC-RPE cells using combinations of C-IV, LN and Nidogen (Nid).

# 2. REVIEW OF LITERATURE

## 2.1 RETINAL PIGMENT EPITHELIUM

### *2.1.1 The structure of the eye and retina*

The basic structure of the eye and retina is presented in Figure 2.1. This thesis concentrates on the back of the eye and more specifically on retinal pigment epithelium (RPE) which will be described later in more detail. There are three layers in the eye wall. The outer layer is a strong and tough sclera, which transforms to a transparent cornea in the front part of the eye. The middle layer is the highly vascular and thin choroid, which contains several pigment cells that averts the reflections coming inside the eye. The inner layer is the retina; a structure, where the light that enters into the eye is focused. Retina consists of two parts: Neural retina, which is the inner layer and RPE, which is the outer layer. Ganglion, bipolar, amacrine and horizontal cells are located in the neural retina. Light needs to penetrate through all these cell types to reach photoreceptors: rods and cones. Optic nerve delivers electric signals from the retina to the brain, where the ultimate picture formation takes place. (Drake et al. 2005; Haug et al. 1995) The cones are highly concentrated in the area called macula, which therefore have the best visual acuity of the retina (Ehrlich et al. 2008). The macula is the central area of the fundus of the eye and comprises a region bounded by the optic nerve and the superior and inferior retinal vascular arcades (Chakravarthy et al. 2010).

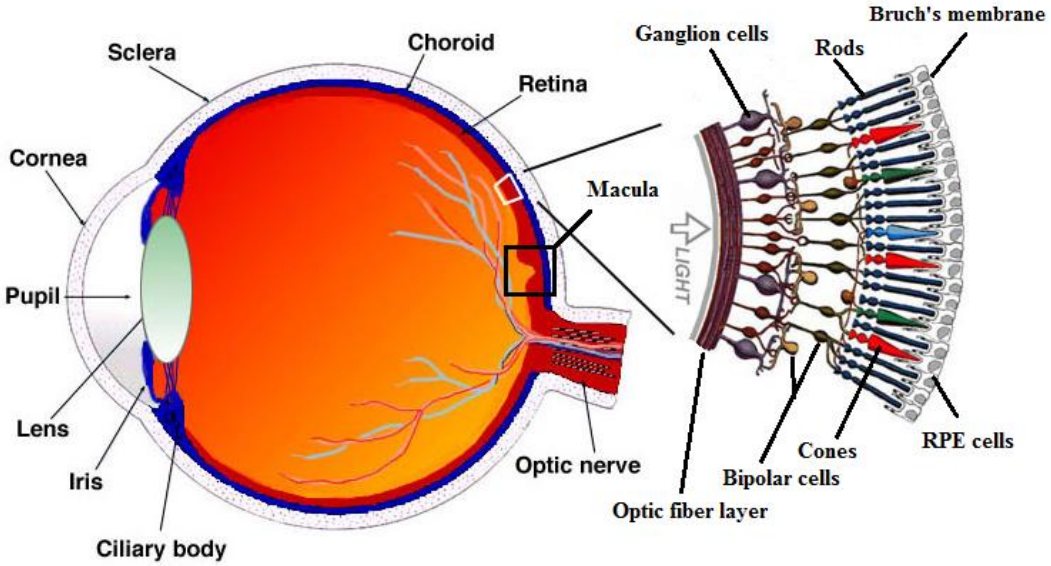


**Figure 2.1** The structure of the eye and the retina. The retina is the innermost surface of the eye. RPE is the outermost layer of the retina and attached to the underlying choroid via Bruch's membrane (modified from WebVision 2011).

### *2.1.2 Retinal pigment epithelium cells*

RPE is a monolayer of pigmented cuboidal epithelial cells located in the retina, at the boundary between bloodstream and the inner eye. The apical membrane contains microvilli and faces the photoreceptor outer segments, whereas the basolateral membrane faces BM which is the structure that separates RPE of the retina from the choriocapillaris of the choroid. (Strauss, 2005) RPE has clear hexagonal morphology which resembles cobblestone-like structure. The color of RPE changes between light brown to black depending on the accumulation of melanin pigment (Figure 2.3). (Maminishkis et al. 2006)

RPE has multiple essential functions that are necessary for normal vision, some of which are shown in Figure 2.2. One of the most important functions of RPE is acting as a protective structure. Each cell of RPE contains high levels of melanin pigment and antioxidants. The melanin filtrates light and prevents photo-oxidation, while antioxidants expedite removal of chemically reactive molecules. (Kevany and Palczewski, 2010) Additionally RPE gives nourishment and support to the photoreceptor cells, forms the blood-retina barrier and especially it has important role in the visual cycle. The function of the visual cycle is to maintain the photoreceptor excitability by regenerating 11-*cis*-retinal from all-*trans*-retinal.

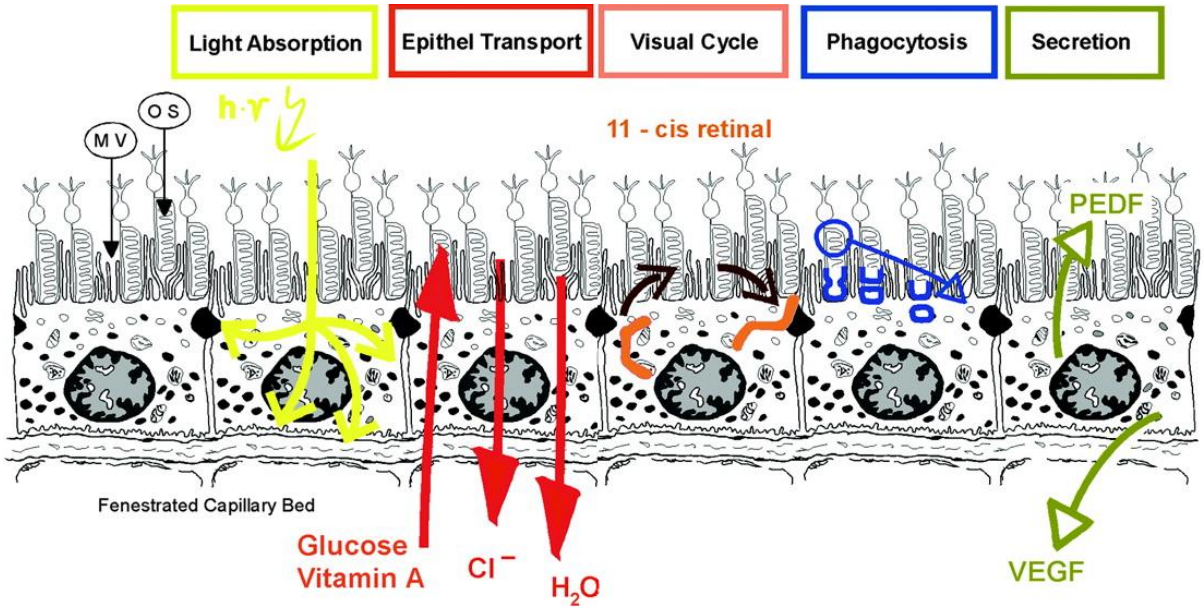


**Figure 2.2** Summary of RPE functions. Acting as a protective barrier by absorption of light into melanin granules, epithelial transport of nutrients to photoreceptors, maintain of visual cycle, phagocytosis of photoreceptor outer segments and secretion of vital growth factors. MV: microvilli, OS: outer segments (modified from Strauss 2005)

Molecule exchange is required between photoreceptors and the RPE because the process cannot take place in the photoreceptors. Phagocytosis of the photoreceptor outer segments (POS) by the RPE is also crucial function in the maintenance of photoreceptor excitability. The POS are digested and recycled as essential substances back to photoreceptors. In addition, the RPE produces and secretes variety of growth factors such as vascular endothelial growth factor (VEGF), pigment epithelium-derived factor (PEDF) and immunosuppressive factors. A failure of any of the functions mentioned can lead to degeneration of the retina and loss of vision. (Strauss, 2005)

### *2.1.3 Characterization of RPE cells*

An electron or confocal microscope is needed in order to visualize the cell polarization, where microvilli are at apical side and basement membrane underlying the epithelium (Maminishkis et al. 2006). Widely used method of characterizing RPE cells is immunocytochemistry, where expression and subcellular localization of specific proteins in the cell are detected. Important molecular markers of mature RPE cells are retinal pigment epithelium-specific protein 65 kDa (RPE65), cellular retinaldehyde-binding protein (CRALBP), $Na^+/K^+$-ATPase, zonula occludens-1 (ZO-1) and claudin-19. One form of RPE65 is cytoplasmic protein that is expressed in the RPE cells. It is involved in visual cycle and associated with retinol binding protein and 11-*cis*-retinol dehydrogenase; furthermore it is involved in vitamin A metabolism, and thus crucial for retinal function. (Al-Hussaini et al. 2008; Ma et al. 2001) CRALBP is associated with normal dark adaptation and it binds to 11-*cis*-retinal or 11-*cis*-retinol in the visual cycle (Saari et al. 2001). RPE differs from other epithelial cells by opposite localization of $Na^+/K^+$-ATPase, which is situated in the apical plasma membrane of RPE cell. The polarization of the cells can be determined by using confocal microscope (Marmorstein, 2001; Sonoda et al. 2009). ZO-1 is a tight junction associated protein that is present in developing and mature RPE cells (Vugler et al. 2008). Claudins are the proteins that determine ion permeability and specificity and especially claudin-19 is a transmembrane protein that is also essential component of human RPE tight junctions (Peng et al. 2011; Rizzolo 2014). The presence of tight junctions can also be determined by measuring transepithelial resistance (TER), which can be calculated from the difference between the resistance of cells cultured on inserts and resistance of inserts without cells (Kubota et al. 2006).

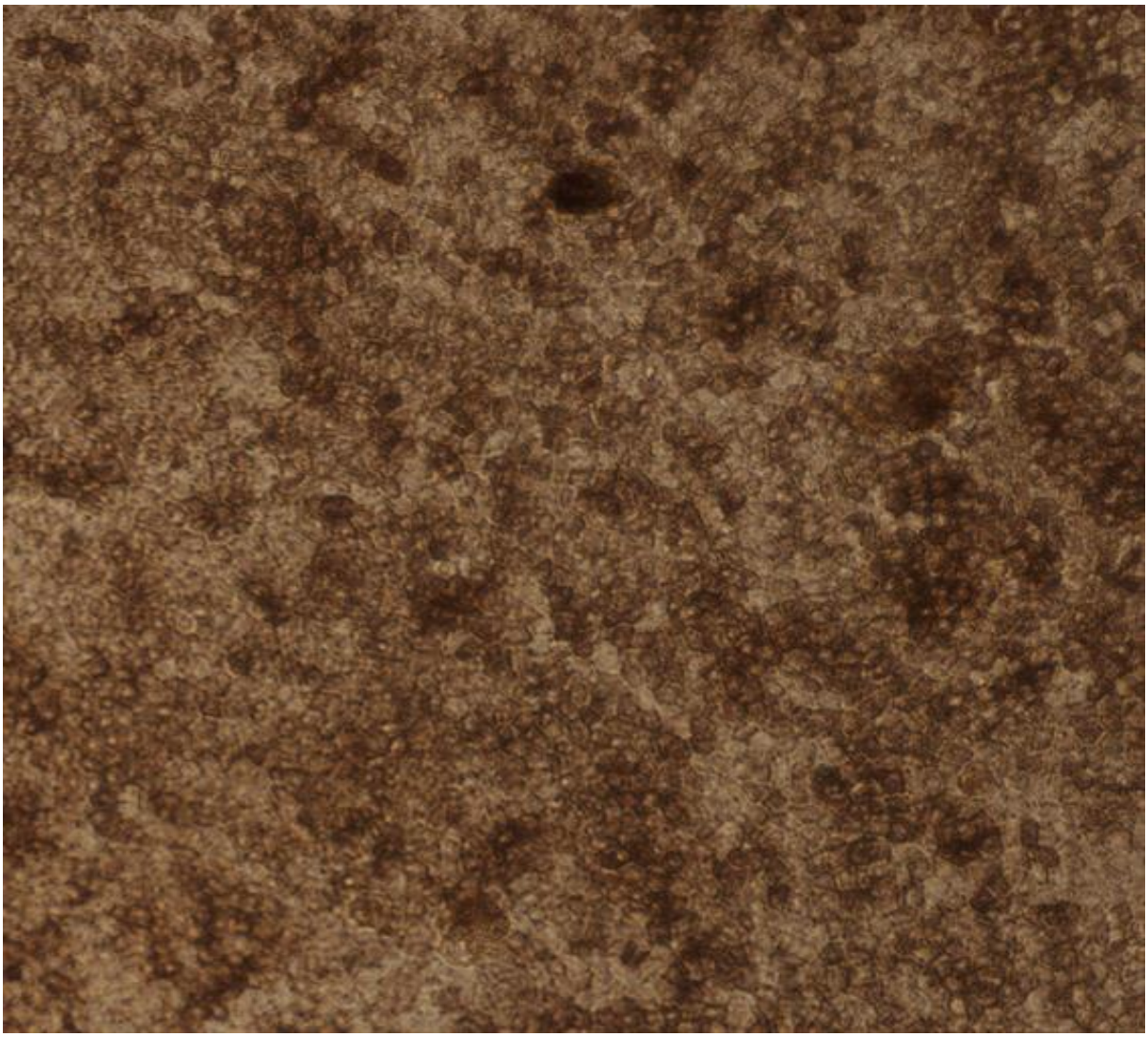

**Figure 2.3** Phase-contrast microscope image with 10x magnification of hESC-RPE cells with representative cobblestone cell morphology and varying degrees of pigmentation

### *2.1.4 Retinal degeneration*

AMD is a progressive degeneration of retina resulting in central visual field loss and ultimately leading to blindness. As its name indicates, AMD affects primarily the elderly, and it is the leading cause of severe vision loss and blindness in people over 60 in the Western countries. (Carr et al. 2009; Jones et al. 2016) There are two different late-stage types of AMD – geographic atrophy and neovascularization. The geographic or "dry" atrophy starts with accumulated waste material in retina which leads to amorphous deposits termed as drusen, this causes RPE to become less pigmented and atrophic; furthermore they are missing in place and stacked up, choroid is degenerated, and deposits form between BM and the RPE layer leading to distortion. This ultimately leads to loss of vision in central areas of the eye

and spreading to other regions. Neovascularization or "wet" exudative type originates from abnormal blood vessel growth through BM, which creates hemorrhage below the macula that does not resorb causing the invasion of the fibrovascular tissue from the choroid and retinal blood vessels. This leakage is devastating for photoreceptors and rapidly leads to loss of vision if left untreated. (Chakravarthy et al. 2010; Chopdar et al. 2003; Lu et al. 2001; Zarbin 2004) The factors leading to AMD are supposed to be combination of genetic disorders and environmental factors involving age, smoking and obesity. Treatment modalities that are used nowadays are a dietary supplementation of anti-oxidants, laser therapy, anti-VEGF, and a combination of laser and anti-VEGF treatment; however these treatments works mainly to the wet type and might still not treat all patients. Moreover, some side effects have occurred with anti-VEGF therapy. Currently, there is no complete recovery from the degeneration. (Kampougeris et al. 2013; Katta et al. 2009)

Another form of RPE-related macular degeneration is Best vitelliform macular dystrophy (BVMD), also called Best disease and caused by faulty *BEST1* gene, which encodes for bestrophin – a calcium-activated chloride channel (Marmorstein et al. 2009; Xiao et al. 2010). Typically BVDM arises in childhood and sometimes in later teenage years. Patients with the Best disease first have normal vision followed by decreased central vision acuity and metamorphosia. Nonetheless, individuals keep normal peripheral vision and dark adaptation. (MacDonald and Lee 2009) Both AMD and BVMD are characterized by an abnormal accumulation of lipofuscin in RPE (Sparrow and Boulton, 2005). It is most likely related to dysfunction in phagocytosis of POS. Lipofuscin disrupts the lysosomal functions of RPE cells and promote their apoptosis leading to retinopathies like BVDM and AMD. (Xiao et al. 2010)

RP is a group of inherited retinal degenerative disorders which is caused by the loss of rod photoreceptors and leads to visual field defects and night blindness. RP is the leading cause of inherited blindness or visual impairment worldwide. It encompasses a number of different manifestations with many distinct genetic causes and diverse biological defects. Many of the genes that are identified to cause RP are involved in the phototransduction cascade, vitamin A metabolism, structural maintenance, cell signaling or interaction. However, the mechanisms of retinal degeneration with RP are still unclear. (Jin et al. 2009) Choriocapillaris and atrophy of RPE are among the classic clinical findings in patients having RP. Several modes of treatments such as gene therapy, injections of neurotrophic factors or anti-apoptotic agents and dietary supplementation are under investigation to slow down the degenerative progress and treat ocular complications. (Musarella and MacDonald 2011)

### *2.1.5 Cell replacement therapies*

Although a number of drugs like anti-VEGF are in use for neovascular AMD, there is currently no treatment for geographic AMD, which is much more common from the two different forms with approximately 80 % of the AMD cases. Nonetheless, replacing dead or dysfunctional RPE with healthy RPE has been shown to rescue photoreceptors from dying and improve vision in animal models. (Nazari et al. 2015) Macular translocation and RPE transplantation surgeries have provided tempting evidence that healthy RPE can support visual function and photoreceptor survival also in human patients with choroidal neovascularization (Binder et al. 2007). Autologous RPE transplantation is accomplished by collecting healthy RPE cells in the peripheral retina and transplanting them into the sub-retinal space at the diseased macula. However, limited autologous sources of maculae and healthy RPE sheets for transplantation in addition with other difficulties such as post-surgery complications, cataract formation and retinal detachment have prevented wide acceptance of autologous transplantation surgeries. (Dang et al. 2015; Nazari et al. 2015)

Since autologous RPE cells have not been reliable enough, researchers have concentrated using more potential sources, such as stem cell-based choices and especially pluripotent stem cells (PSC): human embryonic stem cells (hESC) and human induced pluripotent stem cells (hiPSC). In the last decade, the stem cell-based therapies for retinal degenerative disorders have been mainly focused on three key points: (1) Replacing RPE to maintain the supportive function of the RPE layer, (2) replacement with retinal progenitor cells (RPC) to regenerate lost retinal elements or (3) combining RPE and RPC replacement in advanced stages where both retinal elements and RPE are lost. The ideal methods for efficiently deriving RPE and RPC from PSC for transplantation into the sub-retinal space without immune rejection have been researched extensively. (Nazari et al. 2015) Recently, Miyagishima and co-workers (2016) have presented an autologous iPSC-RPE therapy for clinical applications. They characterized the donor and clonal variation and found that iPSC-RPE function was more significantly affected by the genetic differences between different donors than the epigenetic differences associated with different starting tissues. (Miyagishima et al. 2016)

Differentiating hPSCs to create functional RPE monolayers opened a promising approach to generate virtually unlimited supply of RPE cells (Lund et al. 2006). Thus, differentiation of RPE from hPSCs (hPSC-RPE), which we will be discussed more in the next section, has created a potential solution for a successful cell replacement therapy. Major ethical,

regulatory, safety and technical difficulties have yet to be overcome before stem cell-based therapies can be used in standard treatments. (Nazari et al. 2015) However, the future will be optimistic as there are already ongoing clinical trials using hESC and hiPSC –based RPE cells. (Schwartz et al. 2012; Kamao et al. 2014; www.clinicaltrials.gov, 2016)

## 2.2 PSCs AS SOURCE FOR RPE CELLS

Stem cells are commonly defined as undifferentiated cells that are capable of self-renewal through replication and also capable of differentiation into specific cell lineages. The hierarchy of human stem cells is displayed in the Figure 2.4. Totipotent stem cell can create an entire organism, a property retained by early progeny of the zygote up to the 8-cell stage of the morula. Pluripotent cells, which lie in inner cell mass (ICM) of blastocyst, are capable of forming tissues from embryonic germ layers: endoderm, mesoderm and ectoderm. Multipotent stem cells can yield a bit more restricted group of cell lineages. Stem cells can be classified as embryonic or adult, depending on the developmental stage from which they were acquired. (Fortier, 2005) Since only hPSCs are used in this study, next section will focus on them.

### *2.2.1 Human pluripotent stem cells*

hPSCs have excellent differentiation potential and thus they are intriguing subject to research. The first derived stem cells were obtained from mouse (Evans and Kaufman, 1981), but not long after the first hESC lines were established (Thomson et al. 1998). hESCs are mainly derived from the ICM of the human embryos cultured to blastocyst stage. The embryos used in hESC research are acquired from *in vitro* fertilization (IVF) clinics where the couples going through IVF treatment may choose if they want to donate unused or poor quality embryos to research. Donors voluntarily consent to the donation of embryos and also no financial compensation is made for the donation. The schematics of the process of creating hPSC from human embryos (hESC) and from adult somatic cells (hiPSC) are presented in figure 2.5. The isolation of the ICM cells involves the use of enzymes and immunosurgery for the removal of trophoectoderm, and then the isolated cells of ICM are propagated on feeder cells or on suitable ECM under feeder-free conditions (Skottman et al. 2006). Some countries have strict regulations for hESC isolation, and prevailing ethical questions cannot be set aside (Davies and DiGirolamo 2010). Thus, alternatives to hESCs have been developed. Human iPSCs are the most potential innovation where somatic cells are reprogrammed to embryonic-like

pluripotent stem cells (Takahashi et al. 2007). However, the latest study has shown that hiPSC donor age is associated with an increased risk of abnormalities in iPSCs, such as exomic mutations or gene-disrupting mutations, several which have been associated with cancer or dysfunction. (Lo Sardo et al. 2016)

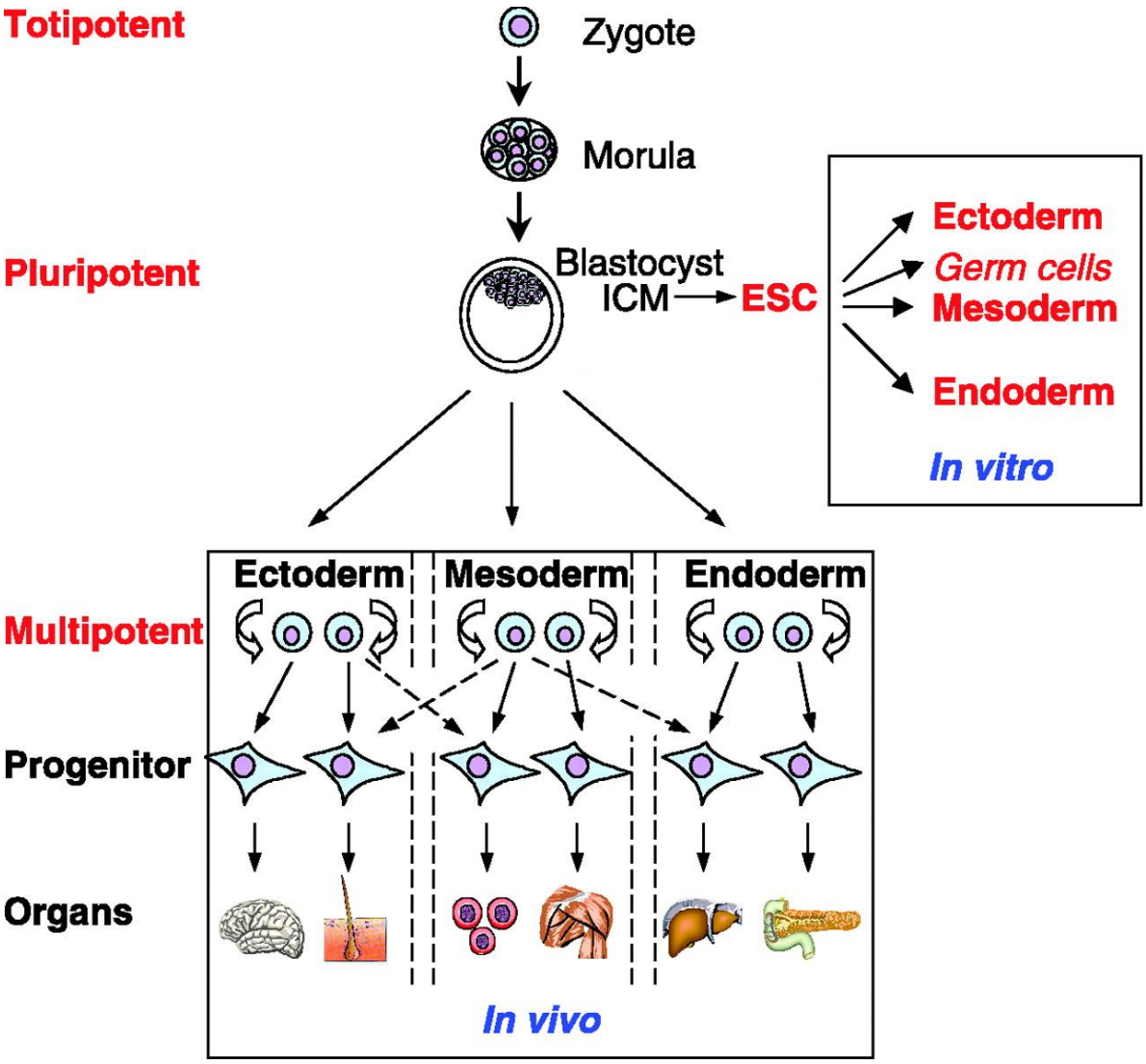


**Figure 2.4** The hierarchy of the human stem cells (modified from Wobus and Boehler 2005)

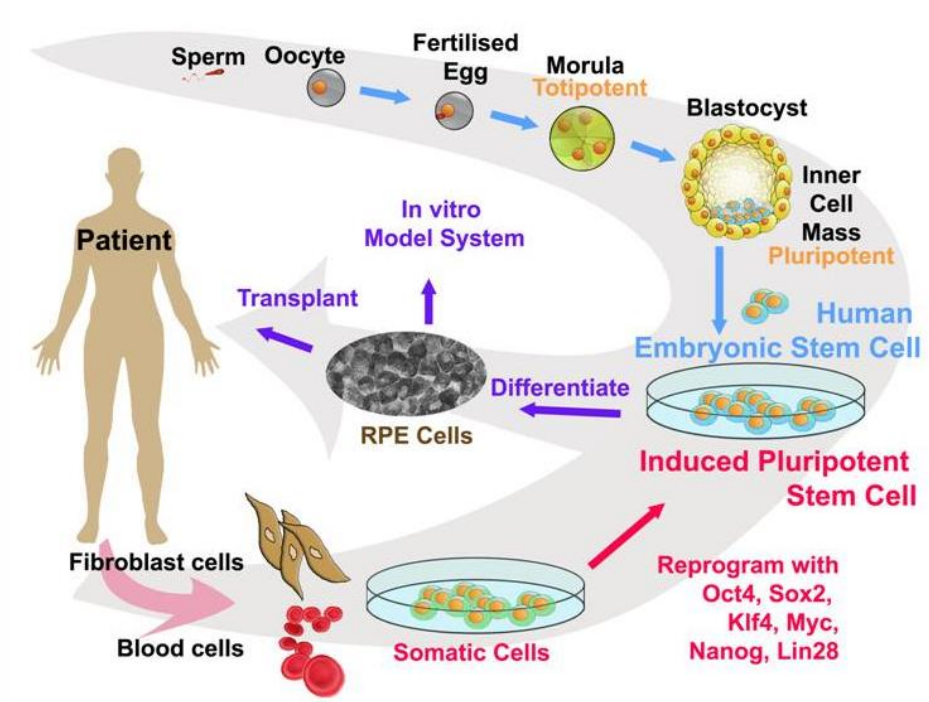


**Figure 2.5** Schematics of the process of creating hPSC from embryos and human fibroblast and blood cells (modified from http://stemcelloverview.weebly.com, 2016 ).

### *2.2.2 Differentiation of hPSCs towards RPE cells*

The first differentiated RPE-like cells from ESCs were reported in 2002 using monkey ESCs (Kawasaki et al. 2002). Current differentiation methods for RPE cells mainly rely on spontaneous differentiation processes favoring neuroectodermal lineage, which is characteristic of hPSCs (Vaajasaari et al. 2011). Using spontaneous differentiation Klimanskaya et al. (2004) initially obtained hPSC-RPE cells by culturing hPSCs on inactivated mouse embryonic fibroblasts (MEFs) and then removing basic fibroblast growth factor (bFGF), which keeps hPSCs in an undifferentiated state, from the culture medium. In the next stage, the cell aggregates start to develop pigmented areas which can be harvested to create monolayer cultures. (Klimanskaya, 2006) These cultures cannot be established on untreated cell culture plastics, because hPSC-RPE cells struggle to adhere to it. Fortunately, the problem can be overcome by coating the cell culture substrate with ECM proteins such as C-IV or LN, both found in BM. (Vugler et al. 2008). Since using bFGF deprivation, RPE-like cells have also been derived through culture on various substrates other than MEFs, including the feeder-free substrate Matrigel and poly-D-lysine-coated dishes. hPSC-RPE differentiation

has been successful using diverse serum-free hPSC culture media, such as Dulbecco's Modified Eagle Medium: Nutrient Mixture F-12 (DMEM/F12) media with knockout serum replacement (KO-SR), mTeSR1 media (StemCell), and XVIVO 10 media (Lonza). The differentiation process takes about 10-12 weeks resulting in numerous pigmented colonies of hexagonal RPE-like cells expressing specific genes. For example, *RPE65*, *CRALBP* and *MERTK* are characteristic to RPE. There are also many other differentiation methods reported, such as two stage induction (Cho et al. 2012), forced induction (Idelson et al. 2009) or rapid differentiation (Buchholz et al. 2013). (Nazari et al. 2015)

It is well known that properties of the existing pluripotent cell lines vary depending on cell line and culture conditions. That is why it is crucial to test RPE differentiation methods and their capacities using several different cell lines. Generation of the RPE cells from hPSCs can be done from pathogen-free cell lines under good manufacturing practice (GMP) conditions. The future of hPSC-RPE relies on xeno-free culture and differentiation process and for example hPSCs have been differentiated successfully towards RPE on human foreskin fibroblasts with KO-SR in differentiation medium. (Idelson et al. 2009; Vaajasaari et al. 2011) Furthermore, feeder-free applications are under research and will become more common in the future.

## 2.3 CELL MATERIAL INTERACTION

Fundamental knowledge of interactions between cells and materials is important for tissue engineering and the development of medical implants. In addition to proper cell culturing substrate, supporting and protective matrix or scaffold is often needed for optimal tissue engineering applications. The cell-material interactions have been studied more in bone grafts and other 3D-implants than 2D-coating materials, but it still can be relatable to explain differences in cell behavior in culture conditions also for hESC-RPE cells. Currently, it is impossible to provide universally optimal coating materials, because the ideal environment varies depending on cell line and culture conditions. Crucial elements when evaluating cell-material interactions are adhesion proteins, cell spreading and material characteristics. (Savioja, 2010; Yli-Perttula et al. 2008; Wilson et al. 2005)

### *2.3.1 Protein adsorption and cell spreading*

The response of the cells to biomaterials is often initiated by cell contact and adhesion to the biomaterial surface. Usually, the cell adhesion to substrates or ECM components is regulated

by proteins that are part of the matrix or have absorbed onto the surface of the biomaterials from the culture media. (Yli-Perttula et al. 2008) The primary interactions between the cells and the adhesion proteins occur via specific transmembrane receptors called integrins, which function as cell surface receptors. (Wilson et al. 2005) LN and collagen (CL) are ECM proteins that interact with specific receptors on the surface of the cells. After adhesion, cells can migrate and divide. The integrin binding of the ECM proteins also initiates the activation of the intercellular adhesive complexes, which is needed for the formation of the cell-cell junctions and functional cell phenotypes. (Yli-Perttula et al. 2008) Cells may change their attachment mechanism by manipulating ECM or adapting to their environment, therefore protein production may alter depending on the culture conditions. These proteins are highly surface active and exhibit high affinity for interfaces. Adsorption may be promoted or opposed by a number of potential enthalpic and entropic changes within surface-media-protein system. These changes depend on the nature of the protein, sorbent and solvent, but they can cause partial dehydration of protein and sorbent surfaces, redistribution of charged groups in the interface or conformational changes in the protein molecule. The intuitive notion is, that the adsorption will increase with time and protein concentration in media normally holds true, at least until the coating approaches the monolayer coverage, which after the adsorption rate decreases in relation of the number of available binding sites, becoming progressively more dependent on the protein-surface affinity. (Wilson et al. 2005)

For a protein to adsorb, both adsorbate and the surface must be at least partially dehydrated, because it is thermodynamically more favorable for similarly hydrophobic sorbents and adsorbates, as it increases the water's entropy. The displacement of water molecules from hydrophilic surfaces is significant energy barrier to protein adsorption. It has been reported that hydrophobic surfaces usually adsorbs more protein than hydrophilic surfaces, likely because they have greater number of possible adsorption-promoting interactions. On top of the dehydration effects, the entropy of the system along with the protein adsorption are affected by the protein's conformational changes, which are the main driving forces for adsorption of proteins to otherwise prohibitive surfaces, such as hydrophilic or carrying a like charge to the protein. The activity of an adsorbed protein varies on its orientation and conformation. (Wilson et al. 2005)

The process of cell spreading is closely related to the cell attachment involving the same ECM proteins. These proteins are needed for the formation of the main contacts and essential intracellular structures. Contractile forces arise from ongoing cell spreading applying tension

to the ECM. These forces can be adequate to displace adsorbed proteins from a biomaterial surface. *In vitro,* many cell types have been shown to depend particularly on adsorbed fibronectin and vitronectin for initial spreading. Thus, the ability of materials to adsorb those proteins from serum is important in sustaining adhesion and the spreading of the cells. (Savioja, 2010; Wilson et al. 2005)

### *2.3.2 Material characteristics*

*In vitro,* the most used material for stem cell cultures is hydrophobic and rigid polystyrene tissue-culture plastic. It is naturally very different from the conditions experienced by the cells in the body, where they are associated with anchored molecules that are surrounding them within an ECM that creates a relatively soft microenvironment. (Lutolf et al. 2009) Despite all reactions depend on cell type and substrates, the properties of the cell culturing materials have great effect on cell attachment. Hydrophilic surfaces are usually superior for cell adhesion compared to hydrophobic surfaces. Thus, some resorbable polymers that are used in tissue engineering are hydrophobic in their native state, and require surface modification or wetting before culturing. (Wilson et al. 2005) For instance coating the surface with C-IV increases the hydrophilicity of the cell culture material (Calejo et al. 2016). Cell membranes carry negative charge and consequently it is presumable that electrostatic interactions will play a role in cell attachment. The mode of cell adhesion is distinct for positive and negative charges. Cell membranes adhere closely to positively charged surfaces, whereas for nearly neutral or negatively charged surfaces there are only distinct contact points. However, despite that the electrostatic attraction between cell membrane and material surface enhances the cell attachment; it does not necessary support cell spreading and differentiation. (Savioja, 2010; Wilson et al. 2005) Since the most commonly used substrata in culturing of the cells are plates with plastic wells and polyethylene terephthalate (PET) membranes, which have often negatively charged surface, it is necessary for anchorage-dependent cells, that have weak attachment to the plastic surface, to produce or attain enough positively charged ECM proteins such as CL or LN from the culture medium. As in this study, coating the surface of the plastic well alleviates the attachment of the cells. (Vancha et al. 2004)

The cell attachment is greatly influenced by surface roughness and topography. Usually, rough surface increases the attachment because disorders and roughness make the surface area larger. They also create confined spaces. It has been speculated that these may interfere with wetting of hydrophobic surfaces and lead to a localized dilution of the coating solution, or

restrict protein exchange between the surface and solution. Cell properties may change due to material interactions. For instance, cell morphology, differentiation, proliferation and motility may vary. Usually if the cell is strongly attached to the surface, cell motility is minor. (Wilson et al. 2005)

Synthetic polymer polyimide (PI) is a material that has been clinically approved and its ocular biocompatibility has been demonstrated, for instance PI membranes have been tested for subretinal transplantation in rats (Julien et al. 2011). In 2012, Subrizi et al. successfully cultured hESC-RPE cells on a transplantable biopolymer PI membrane *in vitro*, although coating with adhesion molecules was needed for cell attachment and spreading. Subsequently, the suitability of ultrathin and porous PI for subretinal transplantation of hESC-RPE was characterized *in vivo* in rabbits, which showed that PI-membrane was well-tolerated in the subretinal space and is a promising scaffold for RPE transplantation. (Ilmarinen et al. 2015)

## 2.4 COATING METHODS AND SUBSTRATES

The basal membrane of anchorage-dependent RPE cells sits on a BM, which is an elastin- and CL-rich ECM that regulates the reciprocal exchange of biomolecules, nutrients, oxygen, fluids, and metabolic waste products between retina and blood circulation. The outermost layer of the BM consists of C-IV, LN, fibronectin, hyaluronic acid, heparin sulfate and chondroitin/dermatan sulfate. Especially C-IV and LN form insoluble networks that both have a structural role, and they also influence the behavior and properties of basal membrane associated cells. In the basement membrane, collateral anchorage of the LN network is provided by the proteoglycans perlecan (PLC) and agrin. A second network is then formed by C-IV, which interacts with the LN network through the heparin sulfate chains of PLC and agrin with additional linkage by Nid. CL and LN are also superior in supporting the adhesion of hPSC-RPE cells on culture surfaces. *In vitro*, the RPE cells need a supportive scaffold and coating that mimic's BM with adequate cell culturing and permeability properties, which has been also the goal for this thesis. (Calejo et al. 2016; Domogatskaya et al. 2012; Hohenester and Yurchenco 2013; Sorkio et al. 2014) In this chapter, the major coating proteins and techniques used in the laboratory experiments of this thesis are introduced. In most cases coating proteins were used in different mixtures to find out the most effective hPSC-RPE maturation substrate. There were two significantly different coating methods used, one being simple DC-protocol and the other was more interesting LS-method.

### *2.4.1 Laminin*

LNs are a family of ECM glycoproteins that are localized in the basement membranes such as BM. LNs are large heterotrimeric cruciform-like structure comprising three disulphide-bonded chains: α, β and γ, which exist in five, four and three genetically distinct forms, respectively. The globular domain at the end of the long arm binds to cellular receptors, including integrins, α-dystroglycan, heparin sulfates and sulfated glycolipids. LN can bind also many of other components of the basement membrane, including C-IV, PLC and Nid, as well as binding itself. LN influence cell function by inducing various signaling pathways via cell membrane receptors. Their primary role is in cell-matrix attachment, but many additional biological activities, such as promoting cell growth, migration, wound repair, and resistance to apoptosis have been demonstrated. (Domogatskaya et al. 2012; Hohenester and Yurchenco 2013; Malinda and Kleinman 1996) Tezel and Del Priore back in the mid 90's showed that tissue culture plastic with LN coating supported human RPE cell attachment more successfully compared to the uncoated ones. Nevertheless, the attachment of the cells was stronger in ECM than LN coated dish. (Tezel and Del Priore 1996) A year later Ho & Del Priore discovered that LN supported better human RPE cell attachment when they compared RPE-derived ECM with LN coated BM and uncoated ones (Ho and Del Priore, 1997). During the last decade, successful and consistent differentiation and maturation of hESCs towards RPE cells on LN coating has been reported (Klimanskaya et al. 2004; Sorkio et al. 2014)

### *2.4.2 Collagen IV*

Unlike most CLs, C-IV is an exclusive member of the basement membranes and through a complex inter- and intramolecular interactions form supramolecular networks that influence cell adhesion, migration and differentiation. In mammals, the C-IV family comprises six highly homologous, yet genetically distinct α-chains. Each chain contains three structurally distinct domains. First is the amino-terminal domain, which is rich in cysteine and lysine residues. It is essential for interchain crosslinking of four triple-helical molecules through disulfide bonds and lysine-hydroxylysine crosslinks. Second domain is a major collagenous Glycine-X-Y triple repeats followed by the third domain, which is a long carboxy-terminal noncollagenous domain. C-IV has one characteristic feature that it has 21-26 interruptions in the collagenous Glycine-X-Y triple repeats. The interruptions provide molecular flexibility for network formation and also serve as cell-binding sites and interchain crosslinking. Once secreted into the ECM, the triple-helical molecules self-associate to form distinct networks providing a molecular scaffold onto witch other ECM components such as LN, PLC, Nid and

proteoglycans can interact. (Khoshnoodi et al. 2008) C-IV coating has been used successfully in consistent differentiation of hPSCs towards RPE cells (Klimanskaya et al. 2004).

### *2.4.3 Nidogen*

The Nid family, also known as entactins, consists of a number of sulfated monomeric glycoproteins ubiquitously present in the basement membrane. Having a wide range of binding partners, they have become considered as adapter proteins in this specialized ECM. Nid-1 has a modular structure with three globular domains G1-G3. G1 is reported to bind C-IV, G2 binds PLC, and G3 binds LN. Because of these interactions, Nids are assumed to stabilize and connect structural proteins in the major networks of the basement membrane such as BM. Even though Nids are ubiquitous elements of the ECM with many binding partners, some genetic analysis has shown that they have no essential purpose for the overall structure of the basement membrane. The role of Nid is rather stabilizing the tissues that are undergoing rapid growth or turnover. (Ho et al 2008) In experiments by Braam et al. hESCs attached poorly to LN+Nid when using defined medium supplements (Braam et al. 2008). Using combination of C-IV, LN and Nid-1 in hPSC-RPE coating is the most interesting aspect in this thesis.

### *2.4.4 Langmuir-Schaefer coating*

Langmuir-Schaefer (LS) method is a developed method from Langmuir-Blodgett (LB) film deposition process, a method, which was first invented by Irving Langmuir and Katherine Blodgett. They discovered that when a solid surface is inserted into an aqueous solution which contains organic moieties, the organic molecules will deposit a homogenous monolayer over the surface. This and other discoveries with surface chemistry merited Langmuir a Nobel Prize in 1932. (Rajvanshi 2008.) The LB technique is an attractive approach for obtaining artificial biomimetic models with a well-characterized molecular organization without the use of bio-incompatible materials or additives. The process is forced to take place at the air-subphase interface in a Langmuir trough, which is a laboratory apparatus that is used to compress monolayers of molecules on the surfaces of a given subphase. The interface is subsequently compressed to obtain oriented molecules and deposited onto a solid substrate. If the deposition of the floating monolayer from the surface of the subphase onto a solid support occurs horizontally, the technique is referred to as LS deposition (Figure 2.6). (Sorkio et al. 2015) Studies have demonstrated that human fibroblasts and adipose-derived stem cells respond well to the oriented rat and calf CL-I films prepared with LB technique (Goffin et al.

2010). Furthermore, the fibroblast cells from human skin have been cultured on LB membranes prepared with CL-I, LN, fibronectin and vitronectin (Higuchi et al. 2002). Sorkio et al. (2015) applied the LS technique to fabricate a biomimetic microenvironment using CL-I and C-IV mimicking the structure and organization of native BM for the production of the clinically relevant hPSC-RPE cells and demonstrated that the prepared LS films have layered structure with oriented fibers and result in increased barrier properties and functionality of hPSC-RPE cells as compared to commonly used DC controls. (Sorkio et al. 2015) Being enthusiastic about these discoveries and by the fact that *in vitro*, LN has been found to self-associate into large polymers (Yurchenco et al. 1985), it was selected as a coating protein for LS coating technique to culture hPSC-RPE cells in this study. The compression of biomolecules in LS technique, which forces them to associate and polymerize with each other's, provides promising possibilities compared to simple DC technique for tissue engineering.

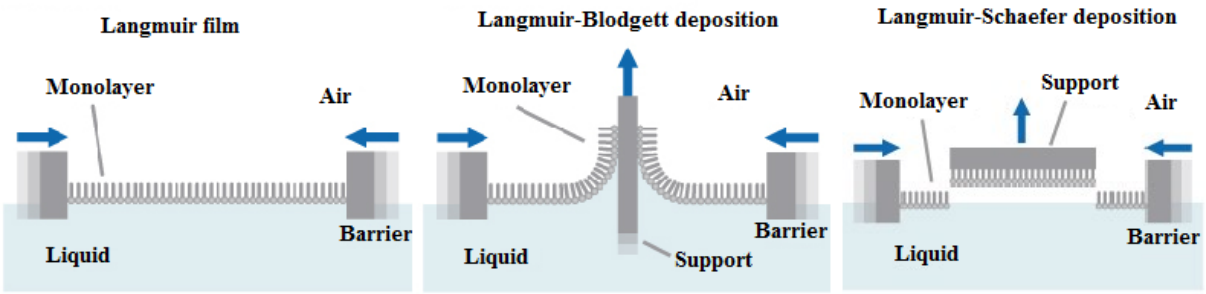


**Figure 2.6** Descriptive picture of the difference of LB and LS deposition methods. (Modified from www.biolinscientific.com)

# 3. AIMS OF THE STUDY

The main goal for this thesis was to find alternative hPSC-RPE cell enrichment and maturation coating for simple C-IV coating, which has major variability problems and often supports cell attachment and spreading weakly. This study examines how the features of LS-coating using LN as a coating protein on different substrate materials have an influence on hPSC-RPE cell culturing and maturation. Furthermore, this study pursues to optimize the best *in vitro* hPSC-RPE cell maturation substrate using combinations of C-IV, LN and Nid. The hypotheses were that the LN would polymerize in the LS-coatings enabling successful hPSC-RPE cell culturing and DC protein combinations would be more successful than previously used C-IV coating.

# 4. MATERIALS AND METHODS

## 4.1 CELL CULTURE ON DIFFERENT COATING MATERIALS

### *4.1.1 DC protocol*

The DC-method's principle is simple: the wanted coating proteins are pipetted straight into the culture inserts in specific concentrations. Commercial PET 24 well (A=0.3 $cm^2$) hanging cell culture inserts with 1 µm pore size (Millipore Corporate, Billerica, USA) were inserted within 24-well plate wells. The membranes of the inserts were coated with different combinations of C-IV (Sigma-Aldrich St. Louis, MO, USA) 5 µg/$cm^2$ per insert, laminin 521 (L521) (Biolamina, Sweden) 1.8 µg/$cm^2$ per insert and Nid-1 (R&D systems, Minneapolis, MN, USA) 0,5 µg/$cm^2$ per insert as a 1x portion (Table 4.1). Coating proteins were diluted with Dulbecco's Phosphate Buffered Saline (DPBS) containing Calsium and Magnesium (Gibco, Waltham, USA) Finally the 24-well plate was wrapped with paraffin and put overnight in 4 °C to wait for cell seeding.

### *4.1.2 LS protocol*

The LS-films were prepared using the KSV minitrough Langmuir film balance (KSV instruments) equipped with a double barrier system. Two fold DPBS with Calsium and Magnesium (in Milli-Q water) was used as a subphase. The temperature of the subphase was 18,0 ± 0,5 °C and the compression speed for the isotherms and Langmuir-film preparation was 65 mm $min^{-1}$ i.e. 48.75 $cm^2$ $min^{-1}$ 180 µl of the 1 mg $ml^{-1}$. 1800 µl of L521 solution was put drop-wise to the same spot on subphase using a glass microsyringe. The film was allowed to equilibrate for 35 min before compression. Then the film was compressed to the deposition pressure of 20 mN $m^{-1}$ and allowed to stabilize for 30 min before deposition on substrates. The compression of the LS films took place symmetrically and horizontally. PET culture inserts with 5 µm pore size (Millipore Corporate, Billerica, USA) and ultrathin, porous PI membrane with 1 µm pore dieameter and 2,2 x $10^7$ pores/$cm^2$ (it4ip, Seneffe, Belgium) were used as a substrate for LS-transfer. The LS-films were transferred onto substrates manually by touch-and-lift method. Then, they were dried in desiccator overnight and then sterilized under ultra violet light for 15 min per each side of the film and hydrated in DM- culture medium for 1 h before passaging the cells.

### *4.1.3 Cell material*

The cell lines used for RPE differentiation in this study were Regea 08/023, Regea 14/010 and Regea 13/012, all hESC lines derived in-house as described before (Skottman 2010), the hESC lines were cultured and differentiated into RPE cells as previously described (Sorkio et al. 2015). All cells were handled in sterile environment and cultured in humidified incubators (Binder, Germany) at 37 °C and 5 % $CO_2$. The same hESC-RPE culture medium (DM-) was used throughout the whole study, it consists of Knock-Out Dulbecco's Modified Eagle Medium (KO-DMEM) supplemented with 15 % KO-SR, 2 mM GlutaMax-I, 0.1 mM 2-mercaptoethanol (all from Gibco, Life Technologies), 1 % Non-essential Amino Acids (NEAA), 50 U/ml Penicillin/Streptomycin (both from Lonza Group Ltd, Basel, Switzerland). The National Authority for Medicolegal Affairs Finland (TEO) has approved research performed with human embryos at Faculty of Medicine and Life Sciences, University of Tampere (Dnro 1426/32/300/05). The Ethical Committee of Pirkanmaa Hospital District supports the derivation of hESC lines from surplus human embryos and their culture for research purposes (R05116).

### *4.1.4 hESC-RPE culture to the coated substrates*

For plating, hESC-RPE cells were washed twice with DPBS after which the cells were detached by adding TrypLE Select (Gibco, Denmark) and incubated 15 min at 37 °C until the cells were loosened. Cell suspension was filtered through 40 µm cell strainer (BD Biosciences, San Jose, USA) into 50 ml Falcon tube with at least 2 ml DM- in it. The single-cell suspension was centrifuged at 1500 rpm for 5 min, after which the supernatant was aspirated and cell pellet resuspended in 1 ml of DM-. Cells were counted by using hemocytometer. 200 000 cells per $cm^2$ were plated on previously DC cell culture inserts or LS-films. Cells were cultured 8, 9 or 15 weeks (Table 4.1). DM- culturing medium was changed three times a week by using aspiration and pipette. Cell attachment, growth, morphology and pigmentation were observed weekly under a phase contrast light microscope (Nikon Corp. Tokyo, Japan).

**Table 4.1** Compilation of experiments in this study

| *Cell line* | *IF staining* | *Coating* | *Technique* | *Material* |
|---|---|---|---|---|
| Regea 08/023 | Day 54 | L521 | LS, DC | PET, PI |
| Regea 14/010 | Day 62 | C-IV, C-IV+L521 | DC | PET |
| Regea 13/012 | Day 62, Day 103 | C-IV, C-IV+L521, C-IV+L521+1x/5xNid | DC | PET |
| Regea 14/010 | Day 64 | C-IV+L521, C-IV+L521+1x/3x/5x/8xNid | DC | PET |

## 4.2 CHARACTERIZATION OF COATING AND CELL MATURATION

### *4.2.1 Detection of protein coating deposition by immunocytochemistry*

Coated cell culture substrates were immunofluorescence stained to inspect the deposition of C-IV and L521 on PET and PI. First, the samples were washed with DPBS and then unspecific binding sites were blocked with 3 % Bovine Serum Albumin (BSA) (Sigma-Aldrich, St. Louis, USA), diluted in DPBS, at room temperature (RT) for 1 h. Next, samples were incubated with primary antibodies RT for 1 h: mouse anti-C-IV 1:200 (Merck Millipore, Darmstad, Germany) and rabbit anti-LN 1:100 (Abcam, Cambridge, UK). Then, samples were washed three times with DPBS and secondary antibodies were diluted 1:500 with 0.5 % BSA-DPBS: Alexa Fluor 568-conjugated (A568) goat anti-rabbit (IgG) and Alexa Fluor 488-conjugated (A488) goat anti-mouse (IgG) (both from Molecular Probes, Termo Fisher Scientific, Waltham, Massachusetts, USA). Samples were incubated at RT for 1h and then washed three times with DPBS. After that, samples were mounted with Vectashield mounting medium (Vector Laboratories Inc., Burlingame, CA, USA) on objective glass and visualized with Olympus IX51 fluorescence microscope (Olympus, Tokyo, Japan). Images were edited using Adobe Photoshop CS4.

### *4.2.2 Intensity test*

8-bit images of the immunofluorescence stained coated substrates were taken with an Olympus IX51 fluorescence microscope. The intensity of the stained C-IV and L521 were measured with ImageJ image processing and analysis software through pixel intensity normalization. The pixel intensities of negative controls were subtracted from the coated samples to remove the background caused by antibodies. Normalization was carried out against the C-IV coated sample. Mann-Whitney U test was performed with IBM SPSS Statistics software for determining statistical significance. P-values under $\leq 0{,}05$ were considered statistically significant.

### *4.2.3 Characterization of hESC-RPE by immunocytochemistry*

At the end points (Table 4.1) the cells were characterized by immunocytochemistry. First, samples were washed tree times with DPBS, fixed with 4 % paraformaldehyde (Sigma-Aldrich) for 10 min at RT, washed three times for 5 min with DPBS and permeabilized with 0.1 % Triton X-100 in DPBS (Sigma-Aldrich) at RT for 10 min. Unspecific binding sites were blocked with 3 % BSA-DPBS at RT for 1 h. Then, the membrane of each cell culture inserts was cut out and divided into four pieces by using scalpel. Next, samples were incubated with primary antibodies (Table 4.2) overnight at 4 °C. All antibody dilutions were prepared using 0.5 % BSA-DPBS. The next day, cells were washed three times for 5 min with DPBS. Then, the secondary antibodies (Table 4.3) were diluted with 0.5 % BSA-DPBS. Samples were incubated in secondary antibody dilutions for 1 h in RT and then washed three times for 5 min with DPBS. 4’,6-diamidino-2-phenylidole (DAPI) included in the Vectashield mounting medium was used for the counter-staining of cell nuclei (Vector Laboratories Inc., Burlingame, CA, USA). The LS-coated hESC-RPE cells (Regea 08/023) were mounted with ProLong Gold Antifade Mountat with DAPI (Molecular Probes, Termo Fisher Scientific, Waltham, Massachusetts, USA). All Staining were visualized with LSM 700 or LSM 780 confocal microscope (both from Carl Zeiss, Jena, Germany) using a 63x oil immersion objective. Images were edited using ZEN 2.1 Black Edition (Carl Zeiss) and Adobe Photoshop CS4.

**Table 4.2.** Used primary antibodies

| ***Antibody*** | ***CAT*** | ***Dilutions*** | ***Host Species*** | ***Manufacturer*** |
|---|---|---|---|---|
| anti-$Na^+/K^+$-ATPase | ab7671 | 1:200 | mouse | Abcam, Cambridge, UK |
| anti-*CRALBP* | ab15051 | 1:500 | mouse | |
| anti-claudin-19 | MAB6970 | 1:100 | mouse | R & D Systems Inc., Minneapolis, MN |
| anti-ZO-1 | 61-7300 | 1:200 | rabbit | Invitrogen |
| anti-RPE65 | - | 1:200 | rabbit | kindly provided by Michael Redmond National Eye Institute, NIH |

**Table 4.3.** Used secondary antibodies

| ***Antibody*** | ***CAT*** | ***Dilutions*** | ***Host Species*** | ***Manufacturer*** |
|---|---|---|---|---|
| Alexa Fluor 568 anti-rabbit | A-11011 | 1:600 | goat | Molecular Probes, Thermo Fisher Scientific, Waltham, Massachusetts, USA |
| Alexa Fluor 488 anti-mouse | A-21202 | 1:600 | donkey | |

### *4.2.4 TER*

The integrity and barrier function of differently coated hESC-RPE culture inserts were studied with TER measurement after 78 days of culture. The measurements were carried out in DM-medium with a Millicell electrical resistance system volt-ohm meter (Merck Millipore, Darmstad, Germany).

# 5. RESULTS

The starting point for this research was to find an alternative and more successful coating protocol for our research group that has previously used DC C-IV to mature hESC-RPE cells. As it can be seen in Figure 5.1, simple C-IV coating was noted as poor option to use, especially on PET membranes routinely used for RPE maturation culture and after cryopreservation, because hESC-RPE formed big pigmented cell aggregates and had slow cell spreading and attachment after replating. A portion of the data in this study is presented in the appendix, due to large number of images.

## 5.1 CELL CULTURE ON LANGMUIR-SCHAEFER AND DIP-COATED LAMININ

### *5.1.1 Deposition of the coating proteins*

Immunocytochemistry was used to investigate polymerization of L521 on PET and PI membrane using LS-technique and DC. In addition, the binding of C-IV to the L521 with Nid was observed (Figure 5.2). Confocal microscope pictures show, that with LS-technique, L521 appeared to be polymerized and attached, especially on PI-membrane, although the polymerization was seen only in certain areas of the sample. There was no clear polymerization seen in DC samples, where L521 was settled down evenly. DC-PET had much stronger staining intensity with anti-LN than DC-PI. C-IV was seen to bind distinctly to L521 in every sample, especially in LS-PI.

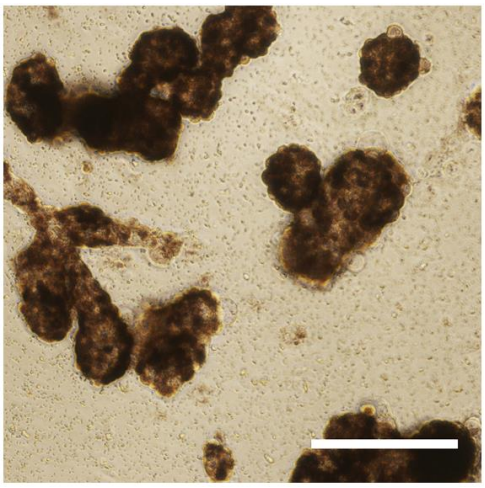

**Figure 5.1** hESCs (Regea 14/010) on C-IV coating cultured 9 weeks in RPE DM- medium. Image taken using Nikon phase contrast light microscope with 10x objective. Scale bar 200 µm.

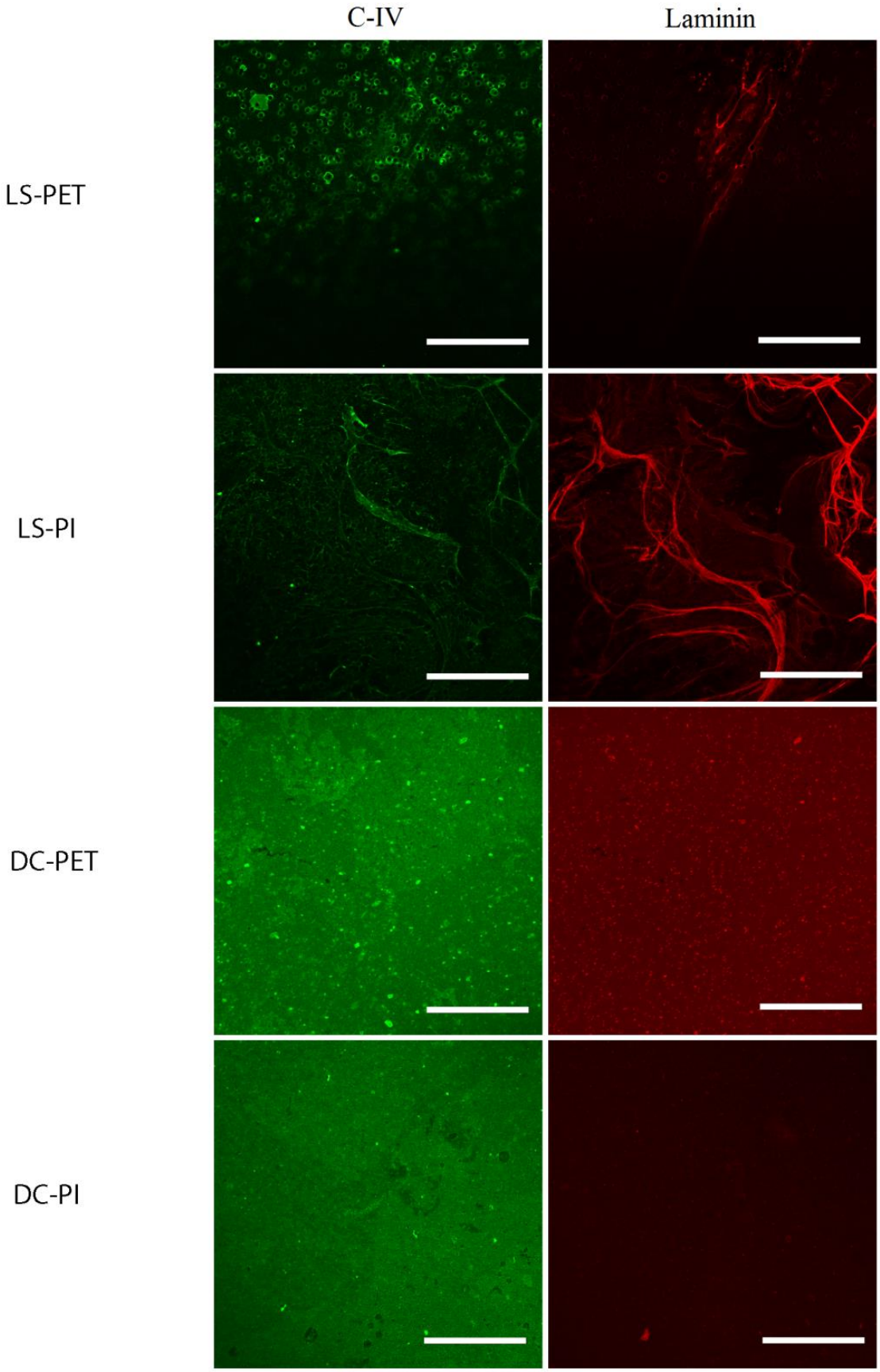


**Figure 5.2** Immunostainings of L521 coated samples using LS- and DC-technique on PET and PI membranes with C-IV and Nid added later using DC-technique. Fluorescence images were acquired with LSM 700 confocal microscope using 20x objective. Scale bar 100 µm.

### *5.1.2 Cell attachment and growth of hESC-RPE on LS-coating*

Since the cell attachment and growth has already been documented on PI using DC LN (Subrizi et al. 2012), DC-PI was dropped out from cell culture experiments and DC-PET was included as control for LS-coating. hESC-RPE cells (Regea 08/023) were cultured for 8 weeks on LS-PET, LS-PI and DC-PET coated with L521. Results concerning to cell attachment and growth can be seen in Figure 5.3. Cell attachment and spreading was clearly faster on DC-PET and cells had also the best morphology and were slightly more pigmented than on LS-PET and on LS-PI. Cells on LS-PI had slightly more pigment than on LS-PET, although on LS-PI pigmentation gets biased in the light micrograph by PI-membrane's yellow color and weaker transparency.

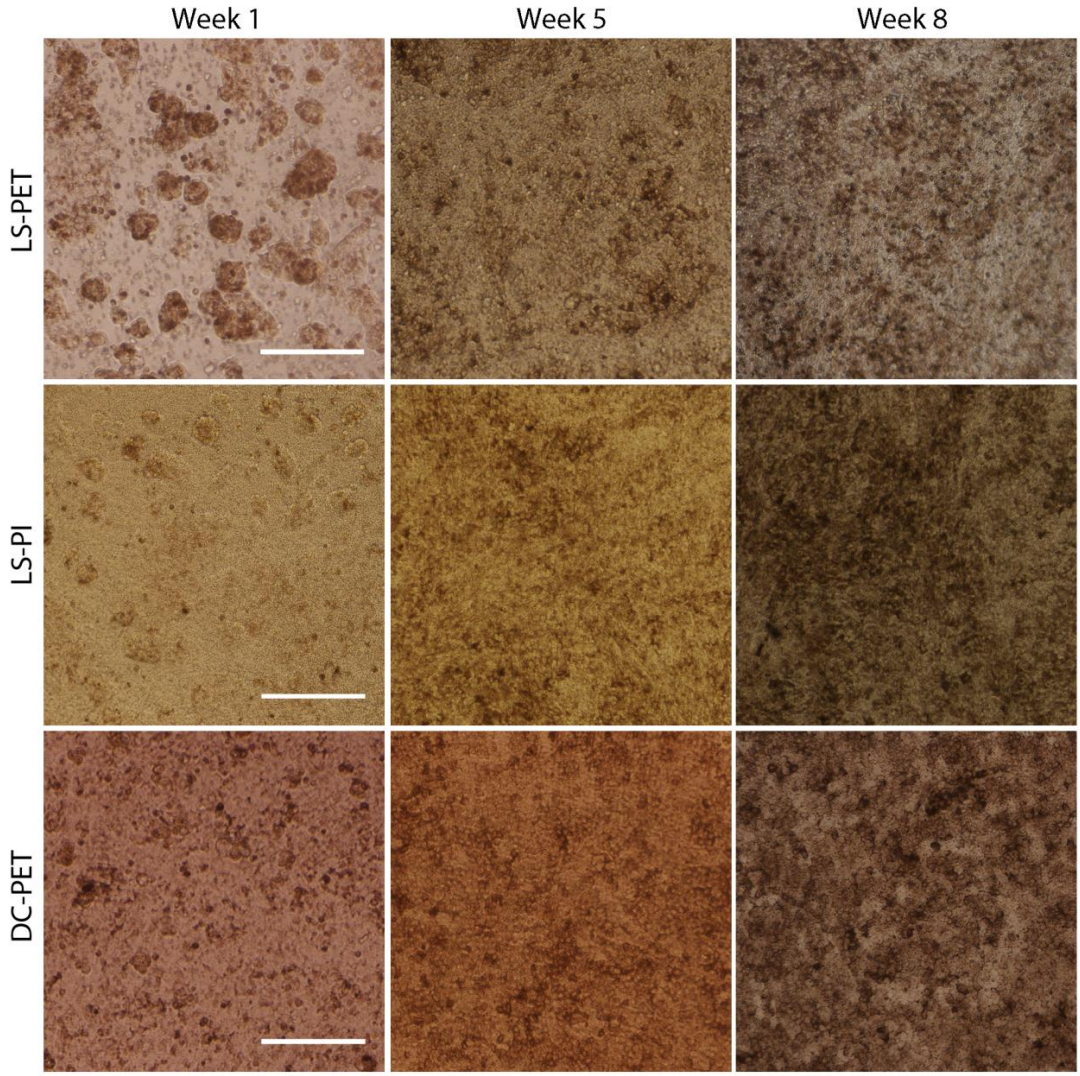


**Figure 5.3** Phase contrast light microscope panel of hESCs (Regea 08/023) cultured in RPE DM- medium using L521 as a coating protein. Coating methods are presented on the left and time points above the picture. Images were acquired with Nikon phase contrast light microscope using a 10x objective. Scale bar 200 µm.

### *5.1.3 Characterization of hESC-RPE on LS-coating with immunocytochemistry*

hESC-RPE, which were cultured for eight weeks, were characterized with immunocytochemistry and imaged with confocal microscopy using z-stacking. The results are presented in Figure 5.4. The cells were clearly very flat in every sample, including the DC-PET control cells. $Na^+/K^+$-ATPase was localized mainly apically in every sample, but in DC-PET cells the localization was better compared to LS-coated samples. ZO-1 showed that cells on LS-PET and LS-PI have cracks between cell membranes. Moreover, it could be seen that ZO-1 was not fully localized to the cell junctions especially in LS-coating samples. Cell membranes in DC-PET are intact and ZO-1 marker is localized more firmly to the cell membranes compared to other samples. Same phenomenon could be also seen in Claudin-19. There is no significant difference between samples in RPE65 or CRALBP. They were all expressed in every sample, although LS-PET has much more background interference than other samples. Altogether, LS-technique did look promising, but unfortunately it needs more research and resources to optimize this technique using LN. DC-PET was chosen for further combination studies to find the best substrate to culture hESC-RPE, since it was the most successfully maturated sample.

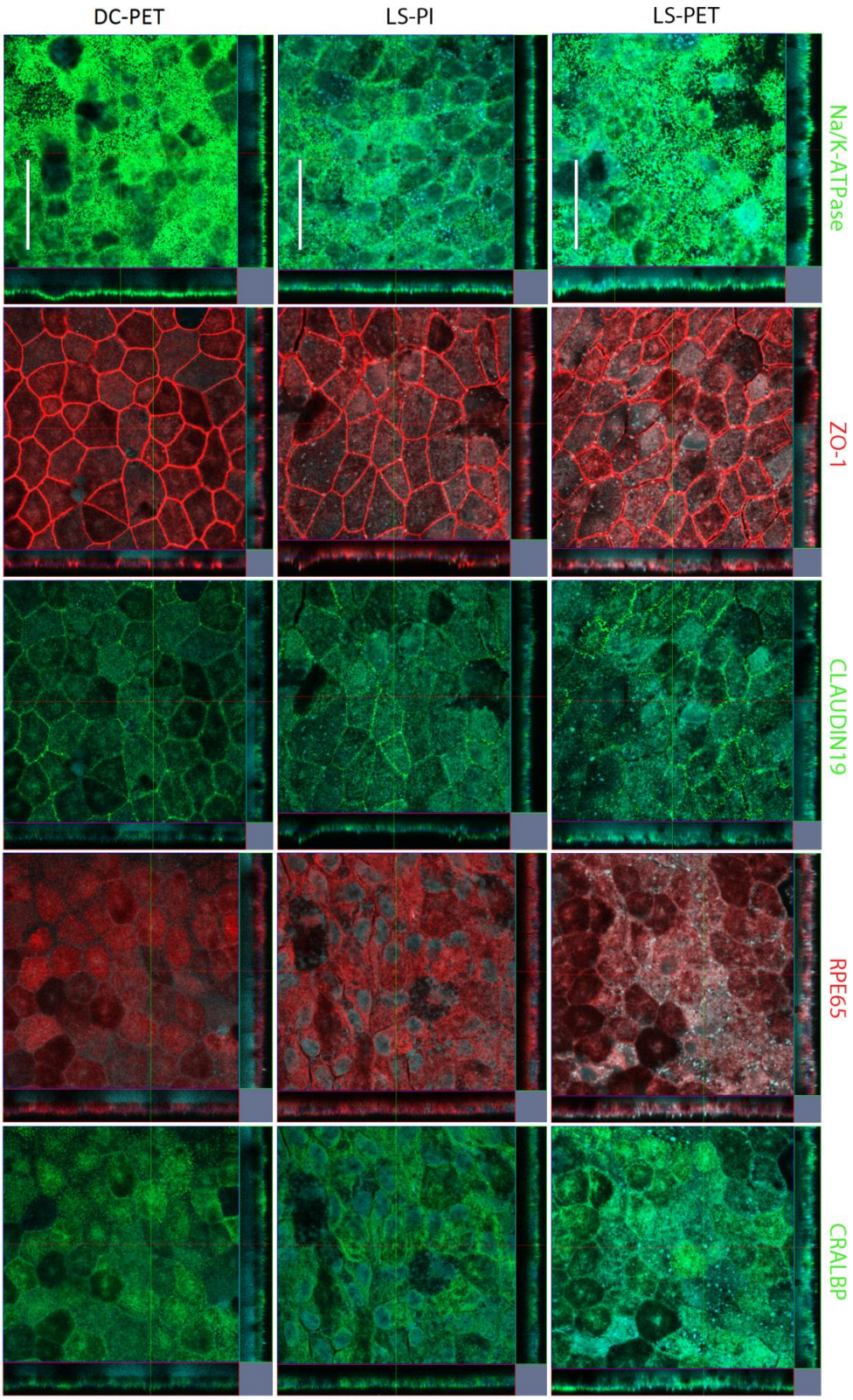


**Figure 5.4** Orthogonal projection images presenting immunocytochemical stainings of hESC-RPE (Regea 08/023) monolayers. $Na^+/K^+$-ATPase, Claudin-19 and CRALBP are presented in green, ZO-1 and RPE65 in red. Every sample was stained with the nuclear counter-staining using DAPI (cyan color). Fluorescence images were acquired with LSM 700 confocal microscope using a 63x oil objective. Scale bar 50 µm. (It is advised to observe the panel horizontally.)

## 5.2 CELL CULTURE ON DIP-COATED PROTEIN COMBINATIONS

First DC combination experimented was C-IV + L521, and it showed great improvement compared to C-IV coating. Cells on C-IV + L521 attached to substrate well and spread fast, they also gained good pigmentation during eight weeks. Furthermore, the cells expressed all the used immunohistochemically analyzed markers (data shown in appendix figure 1). This finding led to the subsequent question whether Nid would further improve hESC-RPE maturation on DC-PET membranes.

### *5.2.1 Deposition of the protein combinations using dip-coating technique*

Immunocytochemistry was used to inspect the deposition of C-IV and L521 using C-IV and LN antibodies. 1x Nid and 5x Nid were added with C-IV and L521 combination to see if Nid had any effects to the deposition. Results are presented in the Figures 5.5 and 5.6. In the C-IV + L521 coating without Nid, there can be seen raft-like areas that indicate probably polymerized L521 with C-IV attached to it. Adding 1x and 5x Nid to the combination caused bright intensity from big aggregates of C-IV and L521. Interestingly, as the intensity test histogram indicates, the more Nid was added, the more C-IV intensity was dispersed. The same phenomenon can be seen in L521 intensity too, but in much smaller magnitude. Especially 5x Nid decreased the intensity dramatically by giving high significance between A488 C-IV and 5x Nid ($P < 0{,}001$), also for A568 C-IV + L521 and 5x Nid ($P = 0{,}001$). However C-IV + L521 and 1x Nid had no significance (A488 $P = 0{,}082$, A568 $P = 0{,}151$)

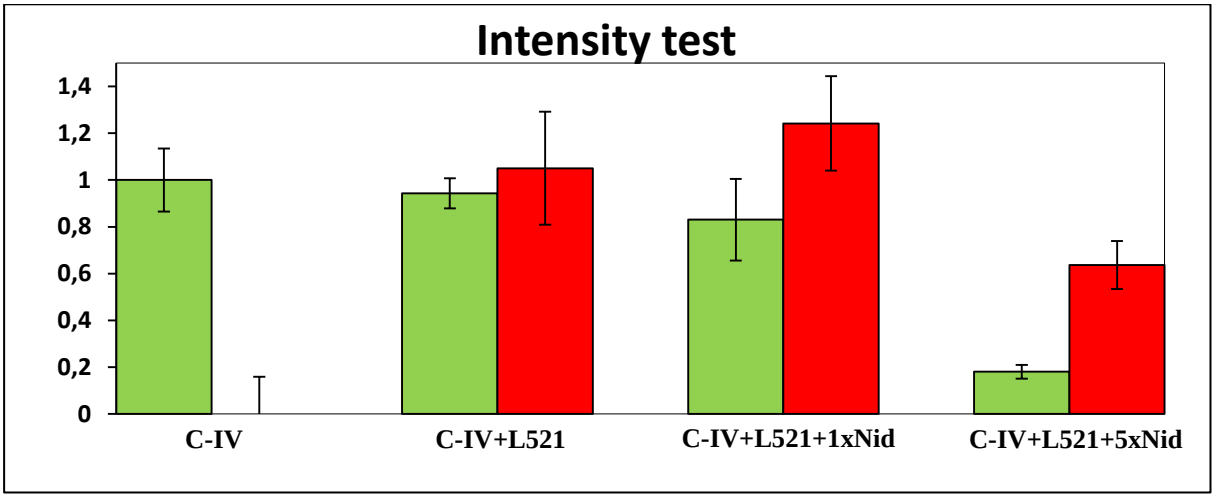


**Figure 5.5** Intensities of anti-C-IV (A488, green column on the left side) and anti-L521 (A568, red column on the right side) on different protein combinations. 10 images were measured from two different samples per protein combination. Background noise was subtracted out and results were normalized against sample, which contained only C-IV. Error bars are standard deviations.

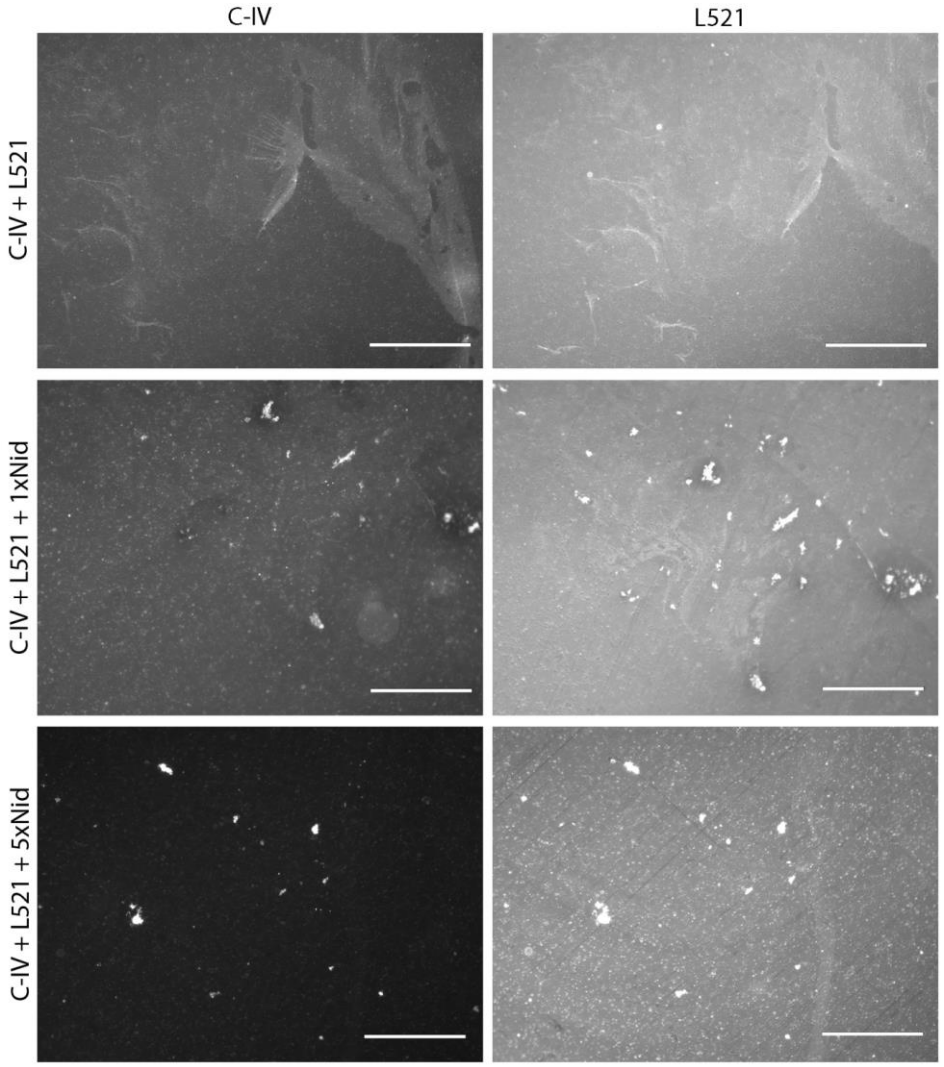


**Figure 5.6** Immunostainings of DC combinations of C-IV, L521 and Nid using anti-C-IV and anti-LN immunofluorescence markers. Protein combinations are presented on the left and fluorescence markers above. Images were acquired with Olympus IX51 fluorescence microscope using a 10x objective. Scale bar 200 µm.

### *5.2.2 Cell attachment and growth of hESC-RPE on DC combinations*

After inspecting the deposition of DC combinations, hESC-RPE (Regea 13/012) cells were cultured on the same coatings for eight and 15 weeks. C-IV coating was also included. Results for eight week culturing are presented in Figure 5.8. Cells plated on C-IV attached and spread much slower than combinations, although compared to previously experiment with DC C-IV (Regea 14/010), the cells succeeded to spread eventually, but occasionally holes were detected in the cell monolayer. C-IV + L521 and C-IV + L521 + 1x Nid looked very similar with each other through the whole 15 weeks. The cells plated on these coatings attached and spread fast but pigmented slower. Cells on C-IV + L521 + 5x Nid coating spread and pigmented also fast but in the first couple of weeks showed small holes in the monolayer

that eventually disappeared. Moreover, cells formed big aggregates, which were attached loosely to the monolayer and ultimately detached during medium changes. After 15 week culturing, all samples looked quite the same, 5x Nid had slightly more pigment than others. Experiment was repeated with another cell line (Regea 14/010), with C-IV + L521 + 3xNid/8xNid coating added and C-IV coating taken out. Results didn't differ significantly from previous experiment; the more Nid was used in the coating, the more pigmentation and floating cell aggregates (figure 5.10 and appendix figure 2). TER values were taken from parallel samples in the week 11. The received values were between 300-370 $\Omega cm^2$ (Figure 5.7), showing no clear trend between different coatings.

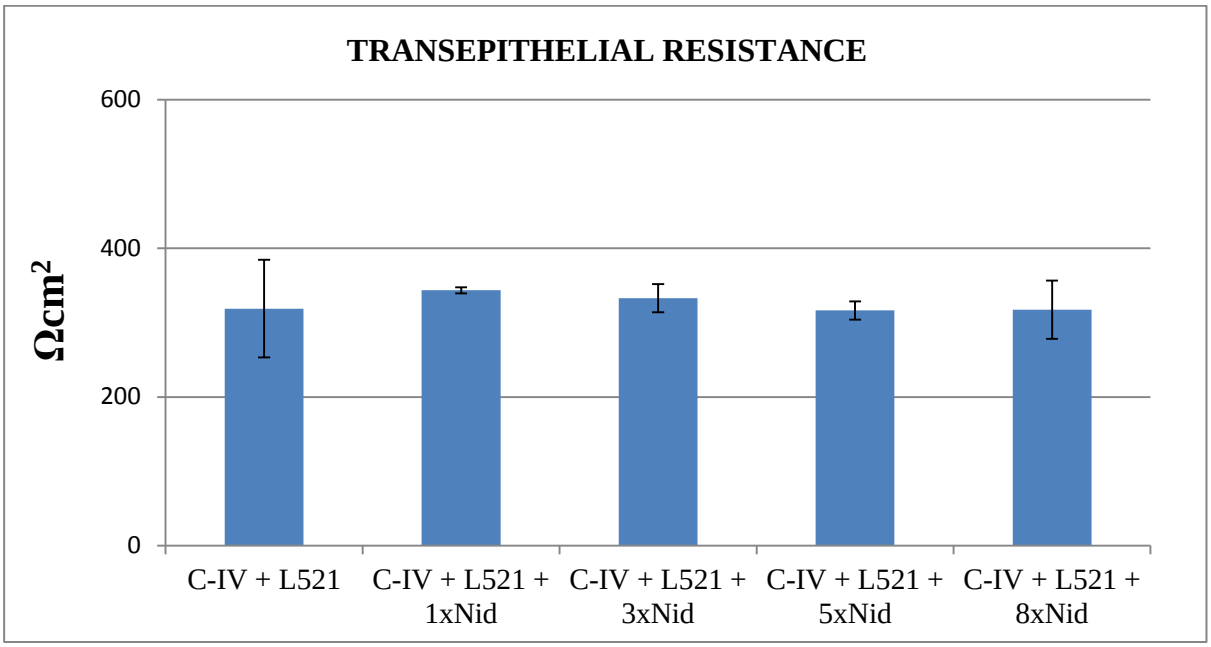


**Figure 5.7** TER of Regea 14/010 RPE-hESC monolayer between different DC combinations presented in Ωcm2 units. Error bars are standard deviations.

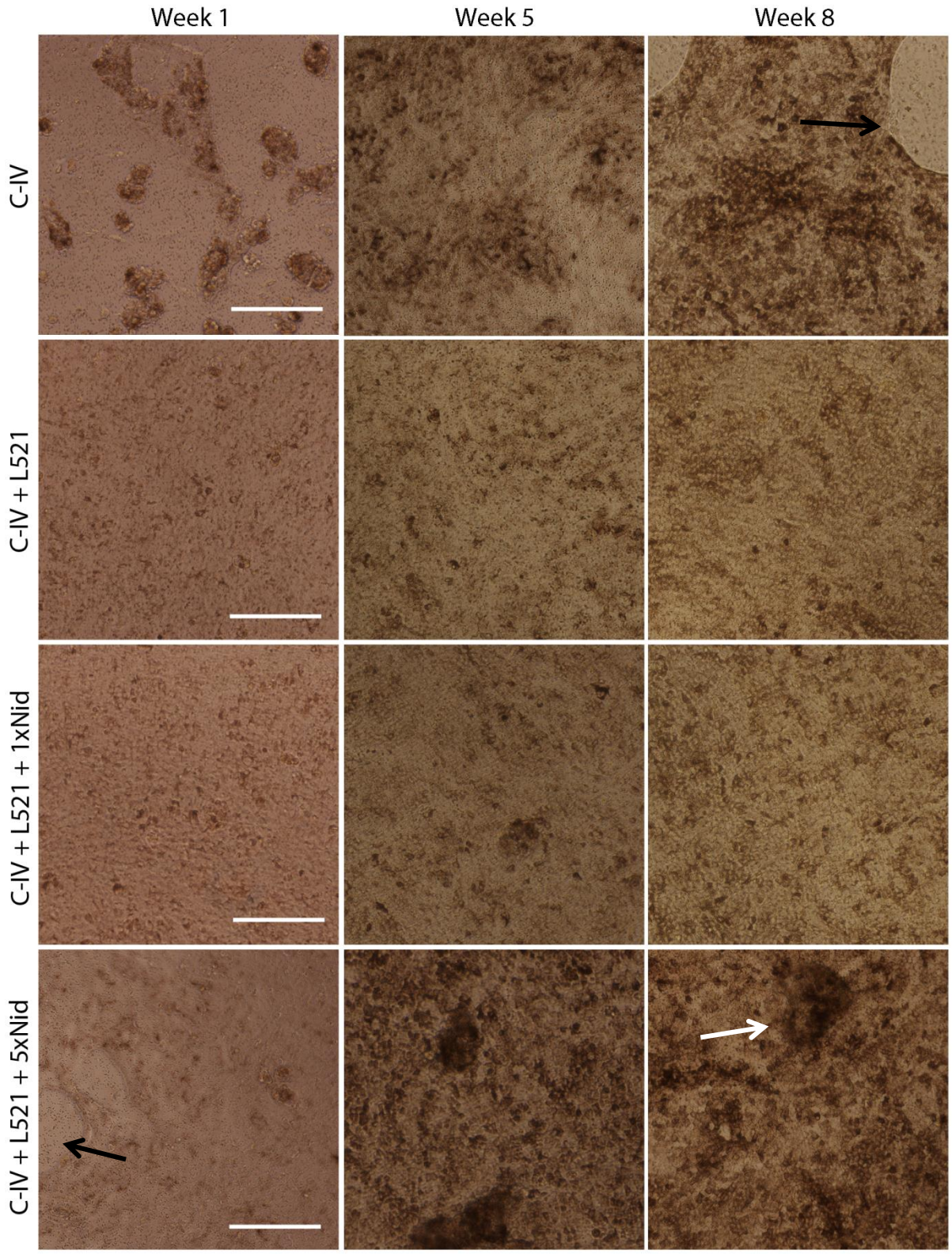


**Figure 5.8** Light micrograph panel of hESC-RPE (Regea 13/012) cultured in RPE DM-medium. DC combinations are presented on the left and time points above the picture. White arrow indicates cell aggregates and black arrows holes in the monolayer. Images were acquired with Nikon phase contrast light microscope using a 10x objective. Scale bar 200 µm.

### *5.2.3 Chracterization of DC hESC-RPE with immunocytochemistry*

hESC-RPE cells on DC combinations were characterized with immunocytochemistry and analyzed with confocal microscopy z-stacking. Immunocytochemical stainings of nine weeks cultured hESC-RPE (Regea 14/010) cells are presented in Figure 5.9 and 5.10. Two end points (9 and 15 weeks) of hESC-RPE diffenrentiated from Regea 13/012 are presented in appendix figures 3-5. However, these results suffered from minor technical problems during the staining procedure and some of the samples had to be re-stained. The intensities are not fully reliable.

hESC-RPE differentiated from Regea 14/010 gave the most distinct results to visualize how the concentration of Nid has an influence on intensity of the immunomarkers. $Na^+/K^+$ATPase was apical in every condition, but revealed that cells on 8xNid showed a slightly different shape than on other coatings. Moreover, the staining intensity in 8xNid sample was lower, but it was also the most pigmented sample. ZO-1 was localized clearly in the cell junctions in every sample. The intensities of claudin-19 increased progressively towards higher Nid concentrations. The same effect is present in RPE65 and CRALBP intensities, as well. Furthermore, the pigmentation of the cells increased in samples with higher Nid concentrations. Claudin-19 samples had small spherical dark spots in the 8xNid sample.

5xNid samples had the brightest claudin-19 intensity in the eight weeks timepoint with hESC-RPE differentiated from Regea 13/012 line but dimmer in the 15 weeks timepoint samples, whereas in places of the C-IV sample, the claudin-19 intensity was brighter compared to combination samples. RPE65 and CRALBP intensities were about the same in every sample in the eight weeks timepoint cells, but in the 15 week timepoint cells, 5xNid had very high intensity in RPE65 and CRALBP compared to other combinations. The $Na^+/K^+$ATPase staining and pigmentation were similar to the results of the hESC-RPE Regea 14/010 cells.

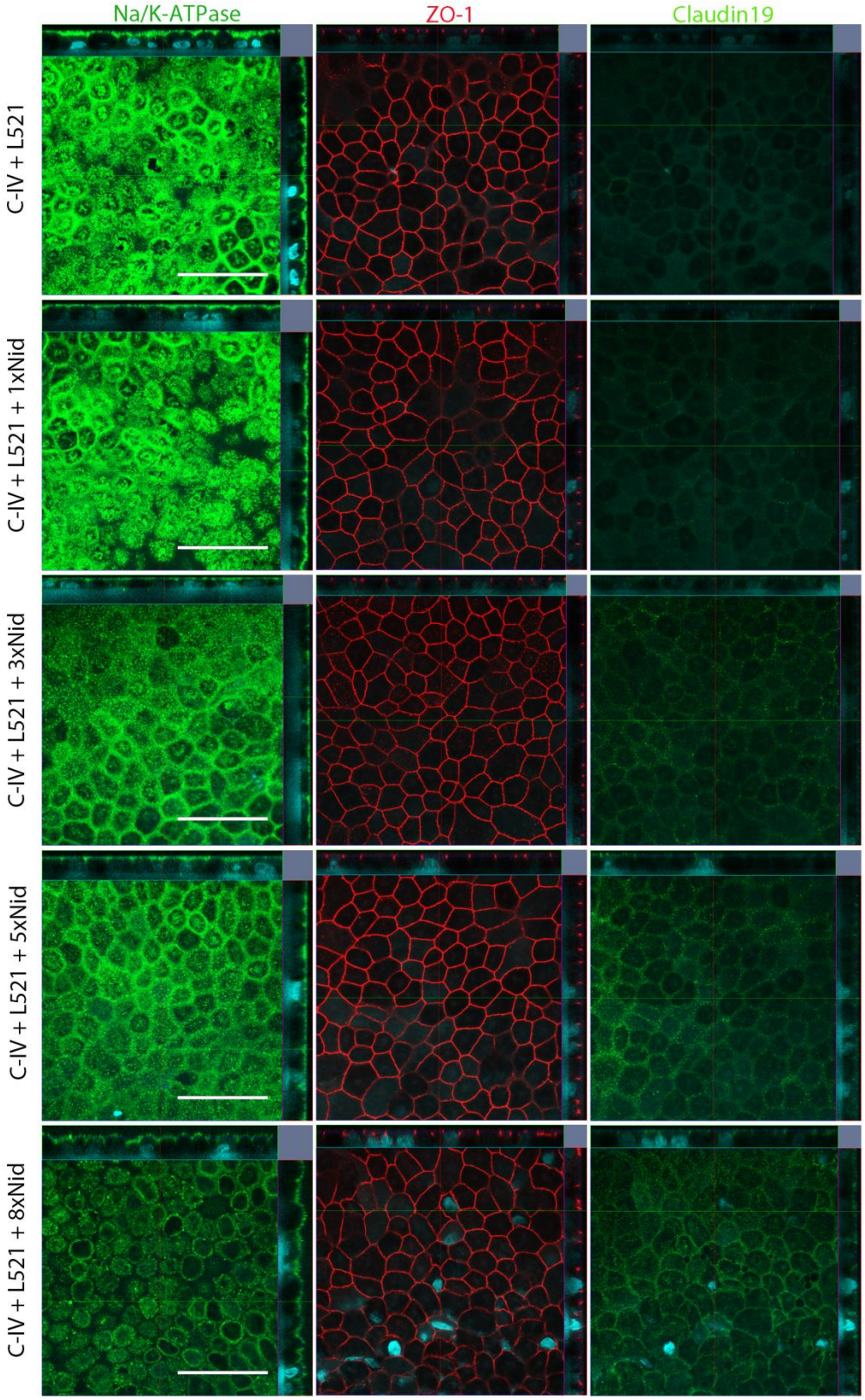


**Figure 5.9** Z-stack images presenting immunocytochemical stainings of hESC-RPE (Regea 14/010) monolayers. $Na^{+}/K^{+}$-ATPase and Claudin-19 are presented in green, ZO-1 in red. Every sample was stained with the nuclear counter-staining using DAPI (cyan color). Fluorescence images were acquired with LSM 780 confocal microscope using a 63x oil objective. Scale bar 50 µm.

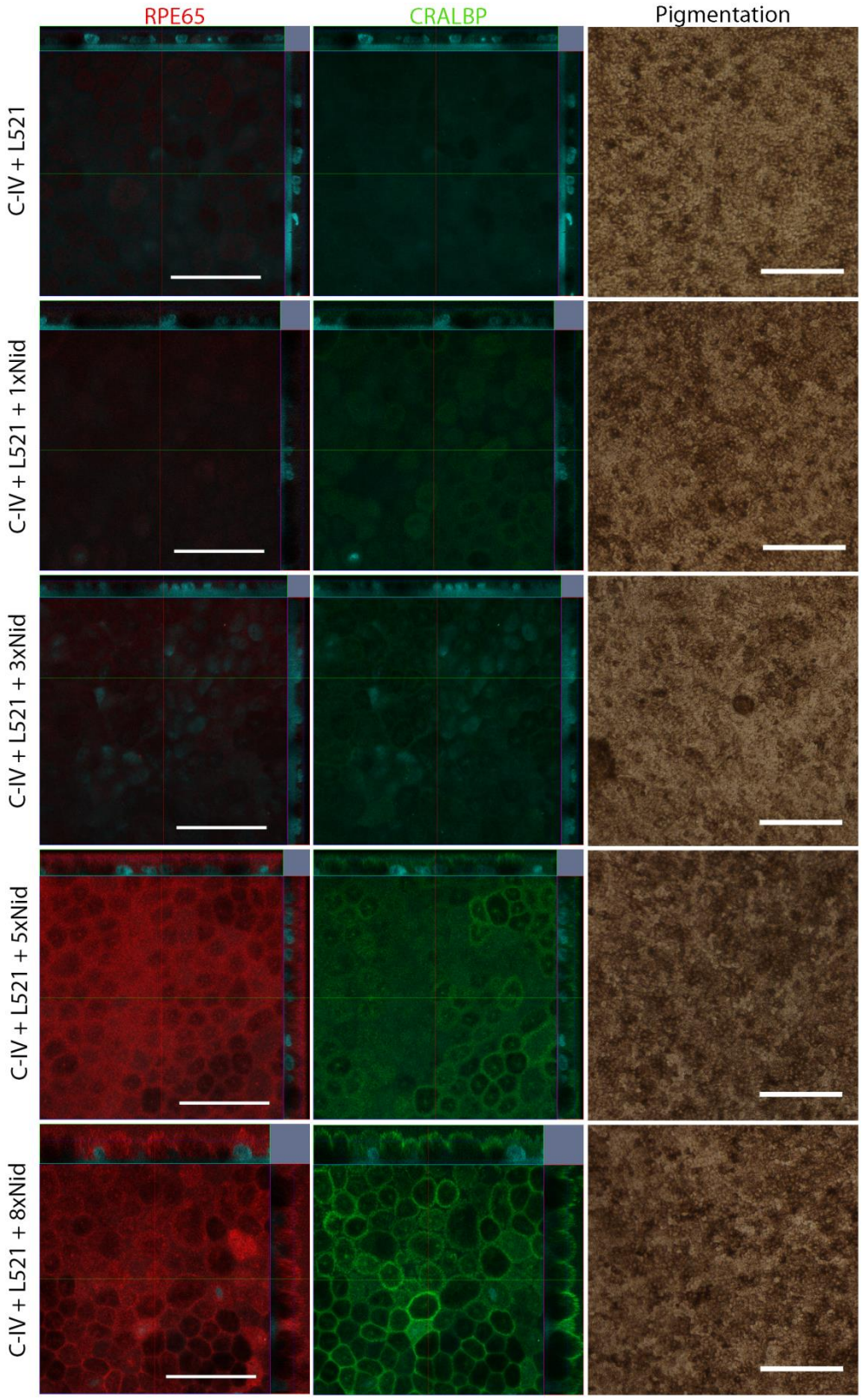


**Figure 5.10** Z-stack images presenting immunocytochemical stainings of hESC-RPE (Regea 14/010) monolayers including cell pigmentation. RPE65 is presented in red and CRALBP in green. Every sample was stained with the nuclear counter-staining using DAPI (cyan color). Fluorescence images were acquired with LSM 780 confocal microscope using a 63x oil objective. Scale bar in RPE65 and CRALBP 50 µm. Pigmentation images were acquired with Nikon phase contrast light microscope using a 10x objective, scale bar 200 µm.

# 6. DISCUSSION

The aim of this study was to investigate different coating methods and thus, try to find an alternative and more preferable coating for hPSC-RPE cell maturation for previously used C-IV coating. This project had two major parts and both of them are discussed here in their own sections. In the first part, the features of LS-technique are compared to DC-method using LN as a coating protein. Furthermore, it was investigated how they affect the hPSC-RPE cell maturation and what are the prospects for the future. In the second part, the best substrate for maturing hPSC-RPE cells *in vitro* was concluded using different combinations of C-IV, L521 and Nid proteins. All in all, the goal for this study was to improve culture conditions for hPSC-RPE cells and moreover, promote RPE research.

## 6.1 CELL CULTURE ON LANGMUIR-SCHAEFER AND DIP-COATED LAMININ

The microenvironments where the cells reside in tissues have great impact on the characteristics of cells including function, morphology and polarity. *In vivo*, the microenvironment of the cells is a combination of multiple complex factors such as the structural environment and ECM. However, many of the classical cell culture substrates do not provide the natural environment for the cultured cells *in vitro*, and moreover, it is difficult to make a substrate that possess similar properties to the tissue environment and that can be produced in a reproducible manner. (Sorkio et al. 2015)

The usage of LB trough as a cell culture coating device is ever so new and interesting approach. Sorkio and co-workers used successfully the LS-coating method to mimic the organized structure and composition of the two uppermost layers of the native BM by using CL-I and C-IV presumably for the first time (Sorkio et al. 2015). That study was also the inspirer for this part of the thesis and since LN is as well very crucial protein of BM and moreover, LS-film formation had not been researched with it before, LS-LN was chosen for this study as hPSC-RPE cell culturing substrate.

The polymerization of L521 on LS-PI membrane was easily confirmed by watching the immunostaining images of the LS-coatings. LS-technique managed to form huge cobweb-like structures of polymerized LN, whereas DC-technique didn’t form any big polymerized

structures. Nevertheless, the LS-PI sample had only a small area that included the polymerized LN and LS-PET had only small fragments of evidence of polymerization. This is probably due to the difficulty to prevent the LN to sink under the surface of the subphase. Furthermore, to pick up the best polymerized areas with touch-and-lift method by hand is not the most optimized technique. Moreover, several samples were noted unsuccessful and only couple of them was used for immunostainings. The variation in the LS-coatings also means that the quality with the samples used in the cell culturing is unknown.

*In vitro*, the cobblestone-like RPE cell morphology, expression of RPE-specific proteins, appropriate subcellular localization of polarized proteins, added with pigmentation and barrier properties of RPE cells are generally considered to be hallmarks of mature RPE. (Sorkio et al. 2014) Considering the hESC-RPE cells cultured in the first experiment, the growth, spreading and gaining of pigmentation were much slower in the LS-coated cell cultures compared to DC control, but eventually they became close to same with the control indicating that it is possible to culture hPSC-RPE cells on LS-coated LN substrate. All samples were superior compared to simple DC C-IV. In previous studies comparing different coating substrates by Sorkio et al. (2014), DC C-IV has been chosen to be the golden midway, although the cell material (e.g. cell line) and whether fresh or cryopreserved cells have been used have big impact to the success of the hPSC-RPE cell maturation.

In immunocytochemical stainings, all the cells in the samples looked very flat, which might have been caused by the staining procedure, because the mounting method was under optimization. The ZO-1 staining showed that LS-coated samples had cracks between the cell membranes and the marker was also slightly spread all over the cytoplasm, rather than staying solely close to tight junctions. Moreover, the claudin-19 staining of the LS samples was also behaving equally with ZO-1. This indicates the maturation might not be complete, although the protocol with the new mounting medium could also be at least partly responsible for that. The cracks between the cell membranes might also be caused by the shrinkage of the cells during fixation or the cells might got dry during the protocol. However, the DC-control was well matured and it had the best morphology. Thus, it was selected for further research with C-IV and Nid combinations. Logistical problems accompanied with resource and timetable issues with the usage of LB trough were another big reason why the DC-technique was chosen for further experiments.

All in all, the formation of LS-coated LN substrates and the culturing of hPSC-RPE cells on them need much more optimization, research and experiments such as TER measurements, gene expression analysis, western blotting and phagocytosis analysis. However, the LS coating technique is a great opportunity for further research and it might become a new application for cell therapy once the procedure is optimized and the best coating protein combinations are found.

Natural continuation for the research would be to fuse C-IV and LN into same LS-protocol and investigate how they polymerize and bind together. It would be also interesting to see how hPSC-RPE cells grow on the LS-coating combination and how it differs from protocol where LS-technique and DC-technique are used with same coating with different combinations. For example, cells could be cultured on the LS-coatings that were used in the protein deposition experiment (Figure 5.2). Now there were not enough samples to do that kind of experiment. In the future, hPSC-RPE cells on the BM mimicking LS-coating on PI-membrane might be transplanted into human's subretinal space and eventually to stop AMD patients to lose their sight. PI-membrane has been already used as a carrier for hPSC-RPE cells in rabbits (Ilmarinen et al. 2015).

## 6.2 CELL CULTURE ON DIP-COATED PROTEIN COMBINATIONS

It is well acknowledged that primary RPE cells are influenced by the surrounding ECM and abnormal ECM can result in altered functions and structure, thus engage in disease states. That is why it is important to compare the effects of different ECM protein coatings on the differentiation and maturation of hPSC-RPE cells. Specifically proteins and protocols, that are most preferably xeno-free, defined or human-sourced and available in GMP-quality. This study pursues these principles, because efficient production of functional, intact and mature sheets of hPSC-RPE cells is considered to be essential for their clinical applications. (Sorkio et al. 2014) However, there are currently many hPSC-RPE differentiation protocols that utilize xeno-derived substrates such as porcine gelatin, even in the clinical setting (Schwartz et al. 2012).

Based on the DC immunostainings (Figure 5.6), it can be seen that L521 was probably polymerized but not as much compared to LS-coatings. The shape of the polymerization resembled rafts and fabrics, whereas when Nid was introduced, big aggregates of L521 were

formed. C-IV was also bound distinctly to L521 structures, but interestingly in 1xNid and especially in 5xNid samples, the overall intensity of anti-C-IV immunomarker became dim, but the aggregated spots were still bright. This outcome suggests that Nid enhances the binding efficiency of the ECM proteins in such way, that big portion of the C-IV is aggregated with L521. The result refers to the fact that Nid connects C-IV to LN (Ho et al. 2008). There is also a chance that Nid covers the epitopes of C-IV, the part in the protein, where the anti-C-IV immunomarker is supposed to bind and thus, the intensity cannot be detected. This theory needs more experiments to be confirmed.

It has been shown, that lightly pigmented cells attach and spread in a substantially greater proportion than more darkly pigmented cells after culture (Schwartz et al. 2012). In this study, this phenomenon could also be seen with C-IV coating, which was more pigmented compared to C-IV + L521 combination, and spread much slower. RPE cells with high degree of pigmentation are considered to be a golden standard for selection of cells for clinical applications (Sorkio et al. 2014). In respect to that statement, it can be seen from the pigmentation panels (Figure 5.8 and 5.10), that 5xNid and 8xNid had significantly more pigmentation in the cells, whereas C-IV + L521 and C-IV + L521 + 1xNid had much less pigment. Furthermore, C-IV + L521 and C-IV + L521 + 1xNid combinations looked approximately the same through the whole study, which indicates that 1x (0,5 µg/cm$^2$) portion of Nid had no major effect in results. C-IV + L521 with or without 1xNid had constantly good growth and spreading, whereas cells on C-IV coating hardly spread at all. On the other hand, higher Nid concentrations (5x and 8x) formed holes in the monolayer in the first two weeks, but after that, the holes closed up quickly and soon, the cell culture started to create big cell aggregates that were partly floating in the culture medium. This phenomenon was witnessed with two different cell lines (Regea 13/012 and 14/010), but the holes in the monolayer mainly in Regea 13/012. 3x Nid had no holes and very few cell aggregates. Regarding to growth, spreading and pigmentation, the effects of the Nid were progressive depending to its concentration.

It is not yet confirmed that the holes and cell aggregates are linked with the aggregated coating proteins in 5xNid samples, but it is high possibility, that these aggregated protein stacks enhances local cell growth, which creates these big cell aggregates. It is also known, that LN enhances adhesion, differentiation, migration and provide resistance to apoptosis (Domogatskaya et al. 2012). If these features are over-expressed locally, it could be a reason for the overgrowth in certain areas. The holes in the early stage of cell culturing could be

explained with the lack of C-IV in 5xNid as the intensity test implies, although it could be also caused by Schwartz and co-worker's (2012) assumption, that highly pigmented cells attach and spread slower. One way to investigate this issue would be an immunostaining procedure, where C-IV and L521 are stained with the nuclei of maturated hPSC-RPE cells, thus it would be possible to observe how the cells are settled with respect to coating. However, it should be always remembered that the difference between cell lines have big impact in the outcome of the maturation.

TER of hPSC-RPE in Sorkio and co-worker's (2014) study was 247±35 $\Omega cm^2$ on C-IV and 128±25 $\Omega cm^2$ on LN. This significantly higher C-IV TER value was one of the most crucial reasons, why C-IV was chosen as the golden midway to hPSC-RPE cell maturation coating, although LN was superior in all other studied aspects. (Sorkio et al. 2014) In this study, TER measurements did not show any significant difference between different coating combinations, indicating that Nid has no effect in barrier properties. This measurement should have been taken also from hPSC-RPE cells cultured in successfully spread C-IV and L521 coatings, because then there would be valid baseline to compare. Furthermore, a negative control measurement, which could be subtracted from the results, taken from empty culture inserts with the same coatings would give more possibilities to analyze results.

The immunocytochemical stainings provided probably the most interesting results regarding the effects of Nid concentration. $Na^+/K^+$-ATPase was apical in every sample regardless of the cell line, indicating that cells are orientated correctly, but it also showed along with RPE65 and CRALBP, that the surface of the hPSC-RPE monolayer in 8xNid sample is much rougher than other samples. This points out, that 8x amount of Nid has probably too much impact in the morphology of the cells. ZO-1 immunomarker is localized in tight junctions in every sample, which advocates the protein combination DC protocol compared to simple LN LS-coating. However, in Sorkio and co-workers (2015) study, LS-coating with C-IV and CL-I had superior ZO-1 expression compared to DC controls (Sorkio et al. 2015). Thus, the successfulness of ZO-1 localization is probably more about the substrate proteins than the LS-coating procedure itself and the synergy between these two aspects. Another tight junction related protein, claudin-19, had progressively stronger expression alongside with the amount of Nid in the coatings, especially in 8 week time point in both cell lines (Regea 13/012 and 14/010). However, in 15 week time point with Regea 13/012, the expression of claudin-19 was decreased, but in C-IV it was the strongest, whereas in 8 week endpoint there was no expression at all in C-IV. This might be caused by the fact, that culturing hPSC-RPE cells for

15 weeks without passaging is quite long time but the C-IV sample was still maturing, whereas coating combination samples were over-aged. Claudin-19 staining had strange small circular dark spots in the 8xNid sample. What produces them is unknown, one possibility is that it is related with the rough surface of the 8xNid monolayer, but these spots might also be something aggregated matter sitting on the cells.

Just like claudin-19, the expression of CRALBP and RPE65 was also progressively increasing with the amount of Nid in the coatings. Especially, when using Regea 14/010 cell line. Regea 13/012 had lesser difference between coatings at 8 week endpoint, but in 15 week endpoint the 5xNid sample was very strongly expressing both immunomarkers. These results, and particularly with Regea 14/010 cell line, indicates that Nid has clear impact in cell maturation, eminently when observing the cell pigmentation and expression of claudin-19, CRALBP and RPE65, that are commonly profiled character of mature RPE. Finding the best combination needs more experiments and methods. For example, more repeats with different cell lines are needed to confirm the results gained in this study. Furthermore different analysis such as quantitative real-time polymerase chain reaction, reverse transcription-polymerase chain reaction, transmission electron microscopy, western blotting and phagocytosis of photoreceptor outer segment analysis alongside with more statistical analysis are needed. As conclusion from this study, the most promising *in vitro* maturing substrate for hPSC-RPE cells would be C-IV + L521 + 3x- to 5xNid on PET inserts. Although, the Nid amount is proportional to the concentration of C-IV and L521 and it might be different for cells that are thawed from cryopreservation, which were not used in this study. Thus, more experiments are needed with thawed cells.

# 7. CONCLUSION

Culturing hPSC-RPE cells has never been completely straightforward process; there are always differences between the cell lines and furthermore, there is great amount of factors that can influence the outcome of the maturing process especially after cryopreservation. For example, simple C-IV coating was considered good in combination with previously used culture conditions, but now that the culture protocols have been otherwise optimized it has become a poor choice, pointing out that the procedure must be reviewed, and that is why this thesis was made.

Using LS-technique as a coating method needs extensively more research and optimization to become a regular coating method for hPSC-RPE cells, but this study showed that LN can be polymerized with LS-method and hPSC-RPE cells can be cultured on it by expressing all the essential immunomarkers and gaining pigment. Results in this study give great opportunity to continue the research once the resources make it possible. For now, the DC method gave much more stable results and showed better and faster maturing process. Thus, it is the better choice for maturing hPSC-RPE cells *in vitro*, but future might change the aspects.

After analyzing the DC combinations, it is certain that C-IV + L521 alone give remarkably better results than previously used C-IV coating, but interestingly the addition of Nid to the combination increased pigmentation and expression of CRALBP, RPE65 and claudin-19. These elements increase progressively alongside the concentration of Nid in the coating. It was also noticed, that Nid caused LN and C-IV to aggregate in the coatings, especially when the concentration was high, indicating the binding properties that Nid protein has with LN and C-IV. Optimizing the right amount of Nid needs more research but rough estimation would be between 1,5 µg/cm$^2$ and 2,5 µg/cm$^2$ of Nid in the coating. Less than that does not show effects in the cells and more than that creates cell aggregates and erratic monolayer.

All in all, this project was successful to denote that NL can be polymerized with LS-technique and DC C-IV, L521 and Nid combinations were approved to be better coating substrate than simple C-IV for maturing hPSC-RPE cells.

# REFERENCES


Al-Hussaini H, Kam JH, Vugler A, Semo M, Jeffery G. Mature retinal pigment epithelium cells are retained in the cell cycle and proliferate in vivo. Mol Vis. 2008;14:1784-91.

Binder S, Stanzel BV, Krebs I, Glittenberg C. Transplantation of the RPE in AMD. Prog Retin Eye Res. 2007;26(5):516-554.

Booij JC, Baas DC, Beisekeeva J, Gorgels TG, Bergen AA. The dynamic nature of Bruch's membrane. Prog Retin Eye Res 2010;29(1):1-18.

Braam SR, Zeinstra L, Litjens S, Ward-van Oostwaard D, van den Brink S, van Laake L, Lebrin F, Kats P, Hochstenbach R, Passier R, Sonnenberg A, Mummery CL. Recombinant vitronectin is a functionally defined substrate that supports human embryonic stem cell self-renewal via alphavbeta5 integrin. Stem Cells. 2008;26(9):2257-65.

Buchholz DE, Pennington BO, Croze RH, Hinman CR, Coffey PJ, Clegg DO. Rapid and efficient directed differentiation of human pluripotent stem cells into retinal pigmented epithelium. Stem Cells Transl Med. 2013;2(5):384-93.

Calejo MT, Ilmarinen T, Jongprasitkul H, Skottman H, Kellomäki M. Honeycomb porous films as permeable scaffold materials for human embryonic stem cell-derived retinal pigment epithelium. J Biomed Mater Res A. 2016;104(7):1646-56.

Carr AJ, Vugler A, Lawrence J, Chen LL, Ahmado A, Chen FK, Semo M, Gias C, da Cruz L, Moore HD, Walsh J. Coffey PJ. Molecular characterization and functional analysis of phagocytosis by human embryonic stem cellderived RPE cells using a novel human retinal assay. Molecular Vision 2009;15:283-95.

Chakravarthy U, Evans J, Rosenfeld PJ. Age related macular degeneration. BMJ 2010;340:526-530.

Cho MS, Kim SJ, Ku SY, Park JH, Lee H, Yoo DH, Park UC, Song SA, Choi YM, Yu HG, 2012. Generation of retinal pigment epithelial cells from human embryonic stem cell-derived spherical neural masses. Stem Cell, 2012;9(2)101-109.

Chopdar A, Chakravarthy U, Verma D. Age related macular degeneration. The British Medical Journal, 2003;326(7387):485–488.

Dang Y, Zhang C, Zhu Y. Stem cell therapies for age-related macular degeneration: the past, present, and future. Clin Interv Aging 2015;14(10):255–264.

Davies SB, DiGirolamo N. Corneal stem cells and their origins: significance in developmental biology. Stem Cells Dev 2010;19:1651-62.

Domogatskaya A, Rodin S, Tryggvason K. Annu Functional diversity of laminins. Rev Cell Dev Biol. 2012;28:523-53.

Drake, R. L., Vogl, W. & Mitchell, A. W. M. 2005. Gray's Anatomy for Students. Elsevier. 1058 pp.

Ehrlich R, Harris A, Kheradiya NS, Winston DM, Ciulla TA, Wirostko B. Age-related macular degeneration and the aging eye. Review. Clinical Interventions in Aging 2008;3(3):473-82.

Evans MJ, Kaufman MH. Establishment in culture of pluripotential cells from mouse embryos. Nature 1981;292(5819):154-156.

Fortier LA. Stem cells: classifications, controversies, and clinical applications. Vet Surg 2005;34:415-23.

Goffin AJ, Rajadas J, Fuller GG. Interfacial flow processing of collagen. Langmuir. 2010;26(5):3514-21.

Hasegawa K, Pomeroy JE, Pera MF. Current technology for the derivation of pluripotent stem cell lines from human embryos. Cell Stem Cell 2010;6(6):521-531.

Haug, E., Sand, O., Sjaastad, Ø. V. & Toverud, K. C. 1995. Ihmisen fysiologia. 1st edition. WSOY. 526 pp.

Higuchi A, Takanashi Y, Ohno T, Asakura T, Cho CS, Akaike T, Hara M. Production of interferon-beta by fibroblast cells on membranes prepared by extracellular matrix proteins. Cytotechnology. 2002;39(3):131-7.

Ho MS, Böse K, Mokkapati S, Nischt R, Smyth N. Nidogens-Extracellular matrix linker molecules. Microsc Res Tech. 2008;71(5):387-95.

Ho TC, Del Priore LV. Reattachment of cultured human retinal pigment epithelium to extracellular matrix and human Bruch's membrane. Invest Ophthalmol Vis Sci. 1997;38(6):1110-8.

Hohenester E, Yurchenco PD. Laminins in basement membrane assembly. Cell Adh Migr. 2013;7(1):56-63.

Hynes RO. The extracellular matrix: not just pretty fibrils. Science 2009;326(5957):1216-9

Idelson M, Alper R, Obolensky A, Ben-Shushan E, Hemo I, Yachimovich-Cohen N, Khaner H, Smith Y, Wiser O, Gropp M, Cohen MA, Even-Ram S, Berman-Zaken Y, Matzrafi L, Rechavi G, Banin E, Reubinoff B. Directed differentiation of human embryonic stem cells into functional retinal pigment epithelium cells. Cell Stem Cell. 2009;5(4):396-408.

Ilmarinen T, Hiidenmaa H, Kööbi P, Nymark S, Sorkio A, Wang JH, Stanzel BV, Thieltges F, Alajuuma P, Oksala O, Kataja M, Uusitalo H, Skottman H. Ultrathin Polyimide Membrane as Cell Carrier for Subretinal Transplantation of Human Embryonic Stem Cell Derived Retinal Pigment Epithelium. PLoS One. 2015;10(11):e0143669.

Jin ZB, Okamoto S, Mandai M, Takahashi M. Induced pluripotent stem cells for retinal degenerative diseases: a new perspective on the challenges. J Genet 2009;88(4):417-424.

Jones BW, Pfeiffer RL, Ferrell WD, Watt CB, Tucker J, Marc RE. Retinal Remodeling and Metabolic Alterations in Human AMD. Front Cell Neurosci. 2016;10:103.

Julien S, Peters T, Ziemssen F, Arango-Gonzalez B, Beck S, Thielecke H, Büth H, Van Vlierberghe S, Sirova M, Rossmann P, Rihova B, Schacht E, Dubruel P, Zrenner E, Schraermeyer U. Implantation of ultrathin, biofunctionalized polyimide membranes into the subretinal space of rats. Biomaterials. 2011;32(16):3890-8.

Kamao H, Mandai M, Okamoto S, Sakai N, Suga A, Sugita S, Kiryu J, Takahashi M. Characterization of human induced pluripotent stem cell-derived retinal pigment epithelium cell sheets aiming for clinical application. Stem Cell Reports 2014;2(2):205–218.

Kampougeris G, Spyropoulos D, Mitropoulou A. Intraocular Pressure rise after Anti-VEGF Treatment: Prevalence, Possible Mechanisms and Correlations. J Curr Glaucoma Pract. 2013;7(1):19-24.

Katta S, Kaur I, Chakrabarti S. The molecular genetic basis of age-related macular degeneration: an overview. Journal of Genetics 2009;88(4):425-49.

Kawasaki H, Suemori H, Mizuseki K, Watanabe K, Urano F, Ichinose H, Haruta M, Takahashi M, Yoshikawa K, Nishikawa S, Nakatsuji N, Sasai Y. Generation of dopaminergic neurons and pigmented epithelia from primate ES cells by stromal cell-derived inducing activity. Proc Natl Acad Sci U S A. 2002;99(3):1580-5.

Kevany BM, Palczewski K. Phagocytosis of retinal rod and cone photoreceptors. Physiology 2010;25(1):8-15.

Khoshnoodi J, Pedchenko V, Hudson BG. Mammalian collagen IV. Microsc Res Tech. 2008;71(5):357-70.

Klimanskaya I, Hipp J, Rezai KA, West M, Atala A, Lanza R. Derivation and comparative assessment of retinal pigment epithelium from human embryonic stem cells using transcriptomics. Cloning Stem Cells 2004;6(3):217-245.

Klimanskaya I. Retinal Pigment Epithelium. Methods Enzymol 2006;418:169-194.

Kubota A, Nishida K, Yamato M, Yang J, Kikuchi A, Okano T, Tano Y. Transplantable retinal pigment epithelial cell sheets for tissue engineering. Biomaterials 2006;27(19):3639-3644.

Lo Sardo V, Ferguson W, Erikson GA, Topol EJ, Baldwin KK, Torkamani A. Influence of donor age on induced pluripotent stem cells. Nat Biotechnol. 2016 Dec 12. [Epub ahead of print]

Lu L, Yaszemski MJ, Mikos AG. Retinal pigment epithelium engineering using synthetic biodegradable polymers. Review. Biomaterials 2001;22(24):3345-55.

Lund RD, Wang S, Klimanskaya I, Holmes T, Ramos-Kelsey R, Lu B, Girman S, Bischoff N, Sauvé Y, Lanza R. Human embryonic stem cell-derived cells rescue visual function in dystrophic RCS rats. Cloning Stem Cells 2006;8(3):189-199.

Lutolf MP, Gilbert PM, Blau HM. Designing materials to direct stem-cell fate. Nature. 2009;462(7272):433-41.

Ma J, Zhang J, Othersen KL, Moiseyev G, Ablonczy Z, Redmond TM, Chen Y, Crouch RK. Expression, purification, and MALDI analysis of RPE65. Invest Ophthalmol Vis Sci. 2001;42(7):1429-35.

MacDonald IM, Lee T. Best Vitelliform Macular Dystrophy. GeneReviews. Updated 12.12.2013. Epub available at: http://www.ncbi.nlm.nih.gov/books/NBK1167. [Cited 3.8.2016].

Malinda KM, Kleinman HK. The laminins. Int J Biochem Cell Biol. 1996;28(9):957-9.

Maminishkis A, Chen S, Jalickee S, Banzon T, Shi G, Wang FE, Ehalt T, Hammer JA, Miller SS. Confluent monolayers of cultured human fetal retinal pigment epithelium exhibit morphology and physiology of native tissue. Invest Ophthalmol Vis Sci 2006;47(8):3612-3624.

Marmorstein AD. The polarity of the retinal pigment epithelium. Traffic 2001;2(12):867-872.

Marmorstein AD, Cross HE, Peachey NS. Functional roles of bestrophins in ocular epithelia. Prog Retin Eye Res 2009;28(3):206-226.

Miyagishima KJ, Wan Q, Corneo B, Sharma R, Lotfi MR, Boles NC, Hua F, Maminishkis A, Zhang C, Blenkinsop T, Khristov V, Jha BS, Memon OS, D'Souza S, Temple S, Miller SS, Bharti K. In Pursuit of Authenticity: Induced Pluripotent Stem Cell-Derived Retinal Pigment Epithelium for Clinical Applications. Stem Cells Transl Med. 2016 Jul 11 [Epub ahead of print].

Musarella MA, MacDonald IM. Current concepts in the treatment of retinitis pigmentosa. J Ophthalmol 2011;753547 Epub avaible at: http://www.hindawi.com/journals/joph/2011/753547. [Cited 3.8.2016].

Nazari H, Zhang L, Zhu D, Chader GJ, Falabella P, Stefanini F, Rowland T, Clegg DO, Kashani AH, Hinton DR, Humayun MS. Stem cell based therapies for age-related macular degeneration: The promises and the challenges. Prog Retin Eye Res. 2015;48:1-39.

Peng S, Rao VS, Adelman RA, Rizzolo LJ. Claudin-19 and the barrier properties of the human retinal pigment epithelium. Invest Ophthalmol Vis Sci. 2011;52(3):1392-403.

Rajvanshi AK. Irving Langmuir - A pioneering industrial physical chemist. Resonance. 2008;13(7):619–626

Reubinoff BE, Pera MF, Fong CY, Trounson A, Bongso A. Embryonic stem cell lines from human blastocysts: somatic differentiation in vitro. Nat Biotechnol. 2000;18(4):399-404.

Rizzolo LJ. Barrier properties of cultured retinal pigment epithelium. Exp Eye Res. 2014;126:16-26.

Saari JC, Nawrot M, Kennedy BN, Garwin GG, Hurley JB, Huang J, Possin DE, Crabb JW. Visual cycle impairment in cellular retinaldehyde binding protein (CRALBP) knockout mice results in delayed dark adaptation. Neuron. 2001;29(3):739-48.

Savioja E. Attachment and differentiation of human embryonic stem cell derived retinal pigment epithelium cells on different coating materials. Master of Science Thesis. Tampere University of Technology. 2010, 77 pages.

Schwartz SD, Hubschman JP, Heilwell G, Franco-Cardenas V, Pan CK, Ostrick RM, Mickunas E, Gay R, Klimanskaya I, Lanza R. Embryonic stem cell trials for macular degeneration: a preliminary report. Lancet 2012;379(9817):713–720.

Skottman H, Dilber MS, Hovatta O. The derivation of clinical-grade human embryonic stem cell lines. FEBS Lett. 2006;580(12):2875-8.

Skottman H. Derivation and characterization of three new human embryonic stem cell lines in Finland. In Vitro Cell Dev Biol Anim. 2010;46(3-4):206-9.

Sonoda S, Sreekumar PG, Kase S, Spee C, Ryan SJ, Kannan R, Hinton DR. Attainment of polarity promotes growth factor secretion by retinal pigment epithelial cells: relevance to age-related macular degeneration. Aging (Albany NY). 2009;2(1):28-42.

Sorkio A, Hongisto H, Kaarniranta K, Uusitalo H, Juuti-Uusitalo K, Skottman H. Structure and barrier properties of human embryonic stem cell-derived retinal pigment epithelial cells are affected by extracellular matrix protein coating. Tissue Eng Part A. 2014;20(3-4):622-34.

Sorkio AE, Vuorimaa-Laukkanen EP, Hakola HM, Liang H, Ujula TA, Valle-Delgado JJ, Österberg M, Yliperttula ML, Skottman H. Biomimetic collagen I and IV double layer Langmuir-Schaefer films as microenvironment for human pluripotent stem cell derived retinal pigment epithelial cells. Biomaterials. 2015;51:257-69.

Strauss O. The retinal pigment epithelium in visual function. Physiol Rev 2005;85(3):845-881.

Subrizi A, Hiidenmaa H, Ilmarinen T, Nymark S, Dubruel P, Uusitalo H, Yliperttula M, Urtti A, Skottman H. Generation of hESC-derived retinal pigment epithelium on biopolymer coated polyimide membranes. Biomaterials. 2012;33(32):8047-54.

Takahashi K, Tanabe K, Ohnuki M, et al. Induction of Pluripotent Stem Cells from Adult Human Fibroblasts by Defined Factors. Cell 2007;131:861-72.

Tezel TH, Del Priore LV. Reattachment to a substrate prevents apoptosis of human retinal pigment epithelium. Graefes Arch Clin Exp Ophthalmol. 1997;235(1):41-7.

Thomson JA, Itskovitz-Eldor J, Shapiro SS, Waknitz MA, Swiergiel JJ, Marshall VS, Jones JM. Embryonic stem cell lines derived from human blastocysts. Science 1998;282(5391):1145-1147.

Vaajasaari H, Ilmarinen T, Juuti-Uusitalo K, Rajala K, Onnela N, Narkilahti S, Suuronen R, Hyttinen J, Uusitalo H, Skottman H. Toward the defined and xeno-free differentiation of functional human pluripotent stem cell-derived retinal pigment epithelial cells. Mol Vis. 2011;17:558-75.

Vancha AR, Govindaraju S, Parsa KV, Jasti M, González-García M, Ballestero RP. Use of polyethyleneimine polymer in cell culture as attachment factor and lipofection enhancer. BMC Biotechnol. 2004;4:23.

Vugler A, Carr AJ, Lawrence J, Chen LL, Burrell K, Wright A, Lundh P, Semo M, Ahmado A, Gias C, da Cruz L, Moore H, Andrews P, Walsh J, Coffey P. Elucidating the phenomenon of HESC-derived RPE: anatomy of cell genesis, expansion and retinal transplantation. Exp Neurol 2008;214(2):347-361.

Wilson CJ, Clegg RE, Leavesley DI, Pearcy MJ. Mediation of biomaterial-cell interactions by adsorbed proteins: a review. Tissue Eng. 2005;11(1-2):1-18.

Wobus AM, Boheler KR. Embryonic stem cells: prospects for developmental biology and cell therapy. Physiol Rev. 2005;85(2):635-78.

Xiao Q, Hartzell HC, Yu K. Bestrophins and retinopathies. Pflugers Arch 2010;460(2):559-569.

Yliperttula M, Chung BG, Navaladi A, Manbachi A, Urtti A. High-throughput screening of cell responses to biomaterials. Eur J Pharm Sci. 2008;35(3):151-60.

Yurchenco PD, Tsilibary EC, Charonis AS, Furthmayr H. Laminin polymerization in vitro. Evidence for a two-step assembly with domain specificity. J Biol Chem. 1985;260(12):7636-44.

Zarbin MA. Current concepts in the pathogenesis of age-related macular degeneration. Archives of Ophthalmology 2004;122(4):598-614.

# APPENDIX

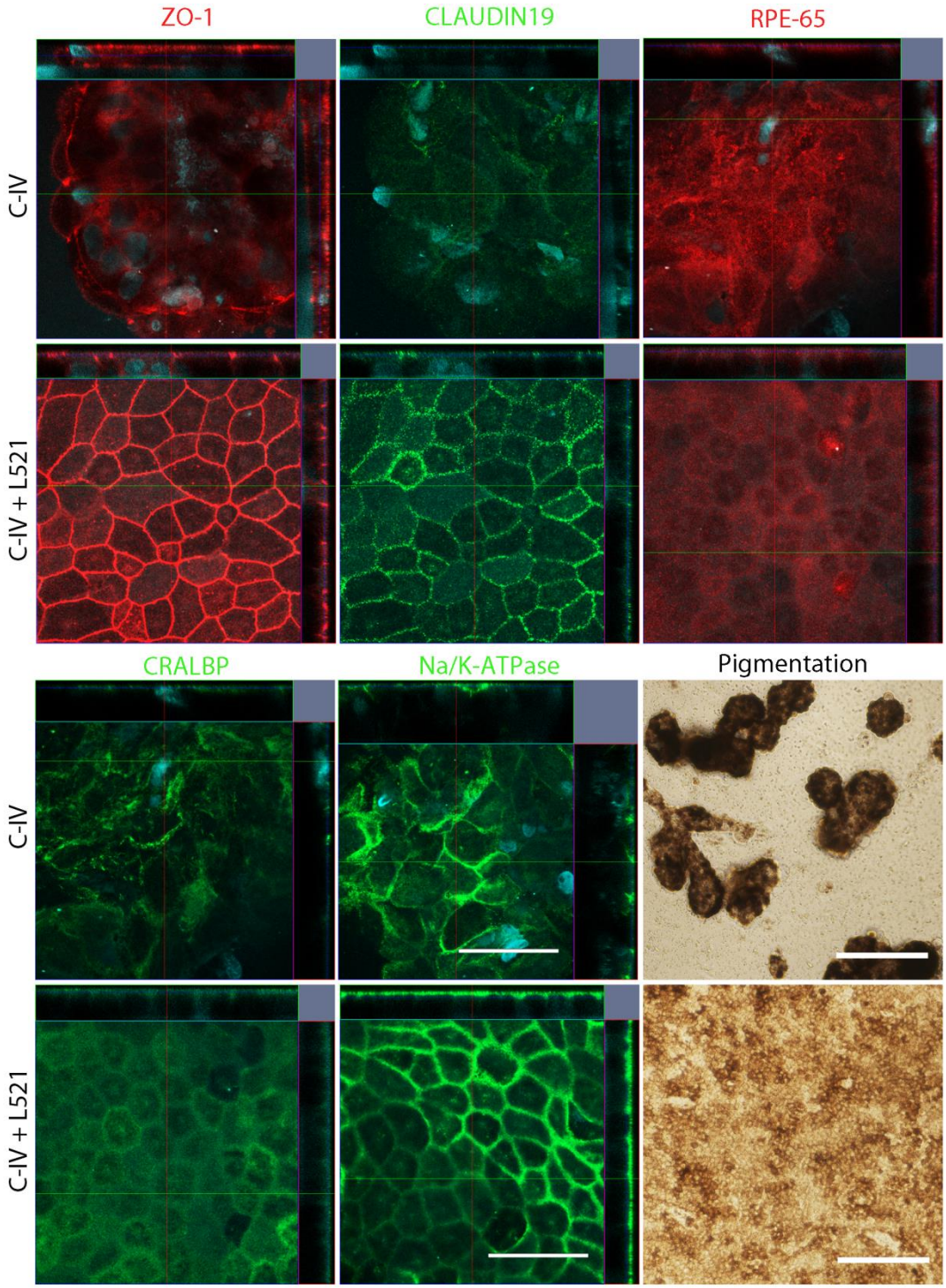


**Appendix figure 1** Z-stack images presenting immunocytochemical stainings of hESC-RPE (Regea 14/010) monolayers with DC C-IV and C-IV + L521. Claudin-19, CRALBP and $Na^{+}/K^{+}$-ATPase are presented in green, ZO-1 and RPE65 in red. Every sample was stained with the nuclear counter-staining using DAPI (cyan color). Fluorescence images were acquired with LSM 700 confocal microscope using a 63x oil objective, scale bar 50 µm. Pigmentation images were acquired with Nikon phase contrast light microscope using a 10x objective, scale bar 200 µm.

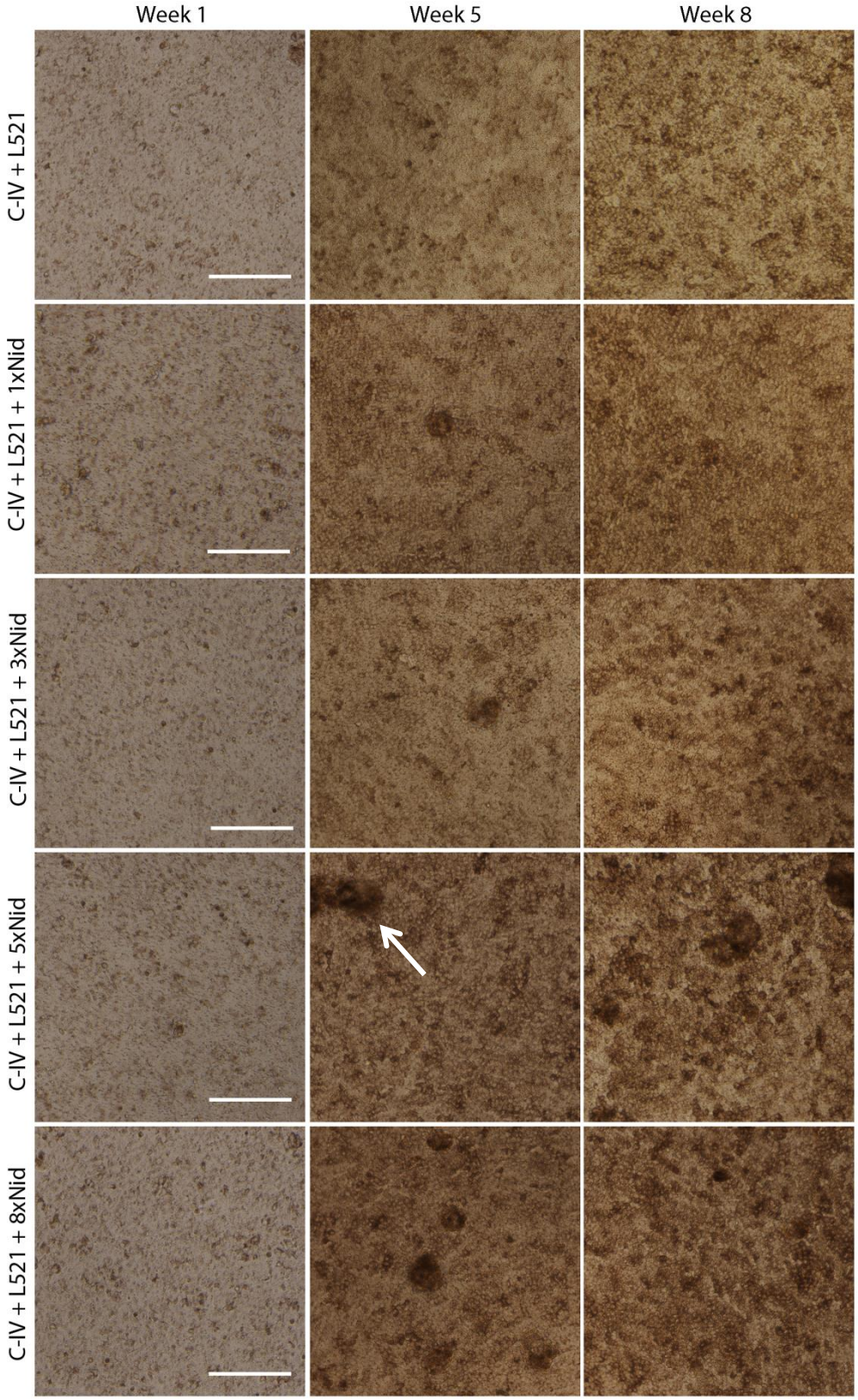


**Appendix figure 2** Light micrograph panel of hESC-RPE (Regea 14/010) cultured in RPE DM- medium. DC combinations are presented on the left and time points above the picture. White arrow indicates cell aggregates. Images were acquired with Nikon phase contrast light microscope using a 10x objective. Scale bar 200 µm.

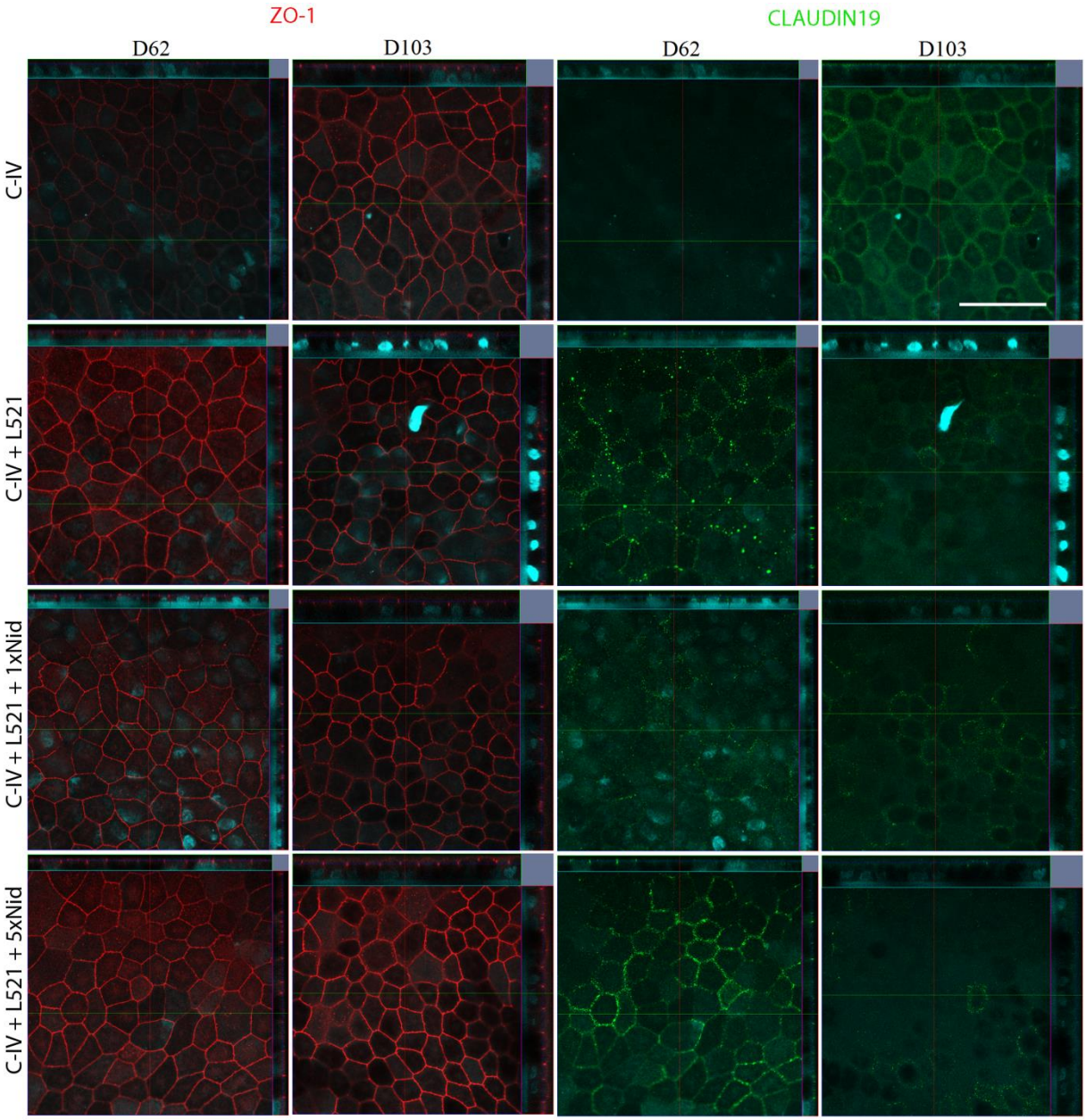


**Appendix figure 3** Z-stack images presenting immunocytochemical stainings of hESC-RPE (Regea 13/012) monolayers in d62 and d103. ZO-1 is presented in red and Claudin-19 in green. Every sample was stained with the nuclear counter-staining using DAPI (cyan color). Fluorescence images were acquired with LSM 700 confocal microscope using a 63x oil objective. Scale bar 50 µm.

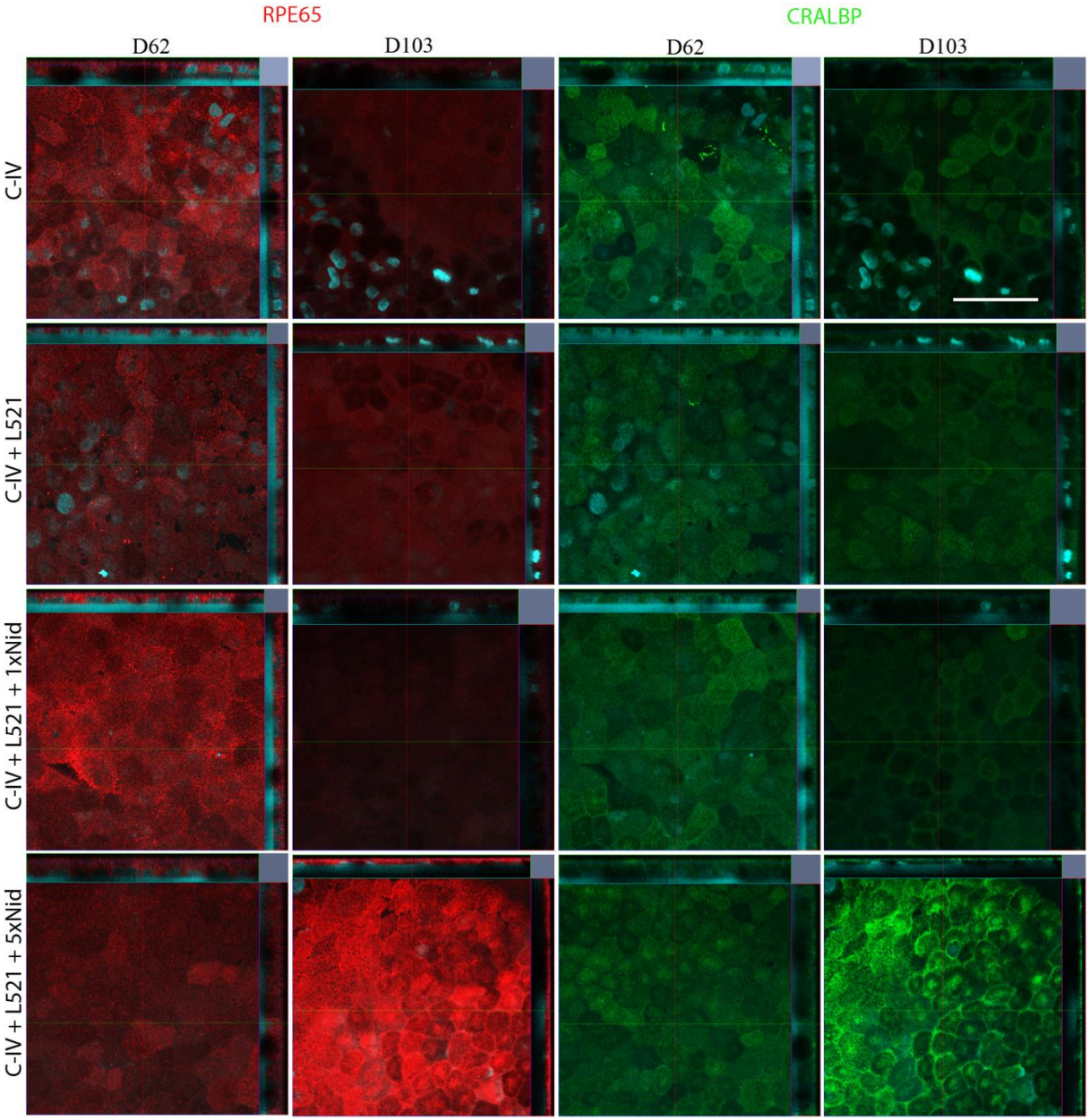


**Appendix figure 4** Z-stack images presenting immunocytochemical stainings of hESC-RPE (Regea 13/012) monolayers in d62 and d103. RPE65 is presented in red and CRALBP in green. Every sample was stained with the nuclear counter-staining using DAPI (cyan color). Fluorescence images were acquired with LSM 700 confocal microscope using a 63x oil objective. Scale bar 50 µm.

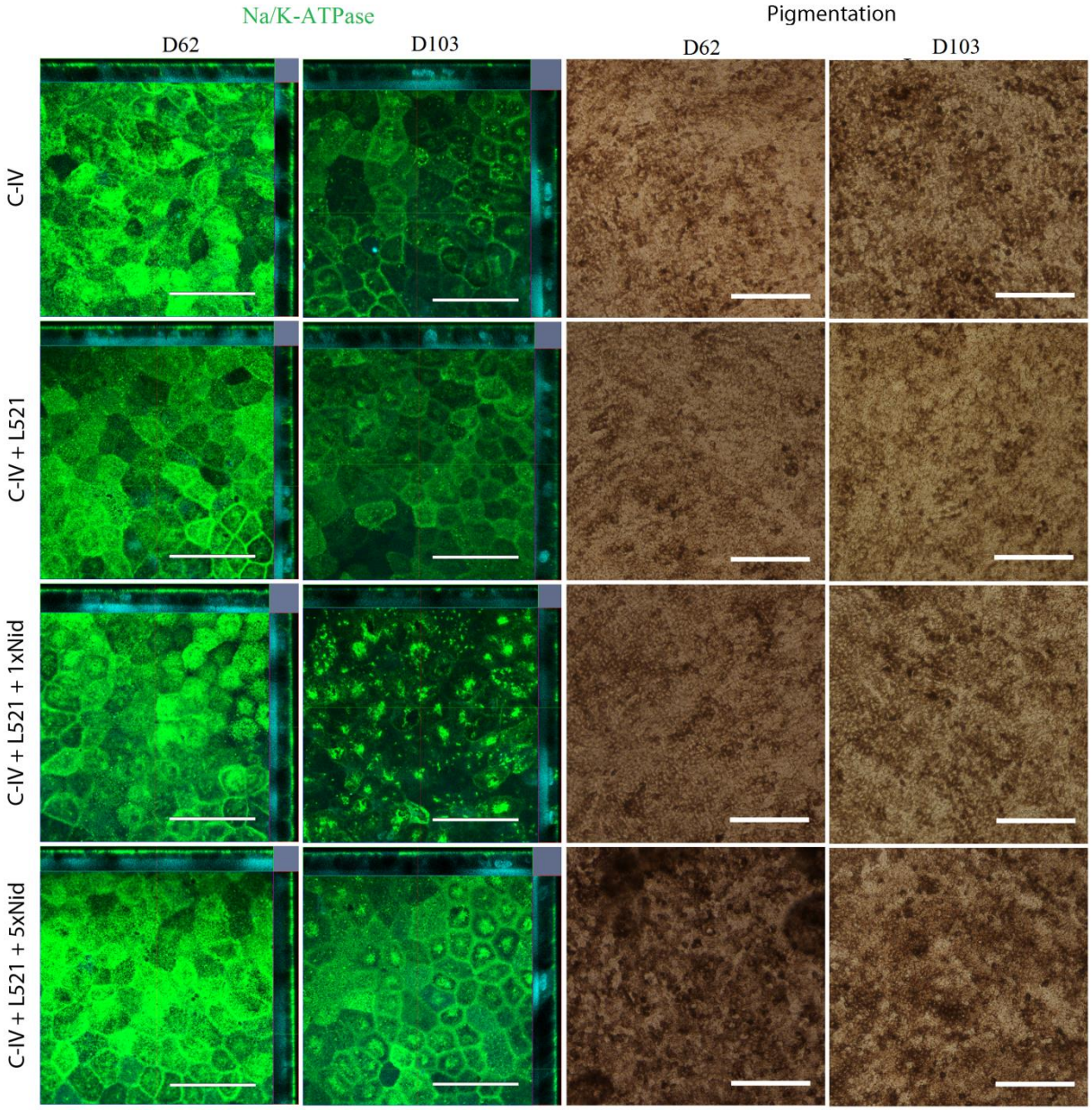


**Appendix figure 5** Z-stack images presenting immunocytochemical stainings of hESC-RPE (Regea 13/012) monolayers in d62 and d103. $Na^+/K^+$-ATPase is presented in green and. Every sample was stained with the nuclear counter-staining using DAPI (cyan color). Fluorescence images were acquired with LSM 700 confocal microscope using a 63x oil objective. Scale bar 50 µm. Pigmentation images presenting pigmentation in d62 and d103. Images were acquired with Nikon phase contrast light microscope using a 10x objective, scale bar 200 µm.